US 20250264412A1

(19) **United States**

(12) **Patent Application Publication** (10) **Pub. No.: US 2025/0264412 A1**

Varnavski et al. (43) **Pub. Date: Aug. 21, 2025**

(54) **TWO-PHOTON FLUORESCENCE MICROSCOPY AT EXTREMELY LOW EXCITATION INTENSITY**

(71) Applicant: **THE REGENTS OF THE UNIVERSITY OF MICHIGAN**, Ann Arbor, MI (US)

(72) Inventors: **Oleg Varnavski**, Ann Arbor, MI (US); **Theodore Goodson, III**, Ann Arbor, MI (US)

(21) Appl. No.: **19/202,888**

(22) Filed: **May 8, 2025**

Related U.S. Application Data

(63) Continuation of application No. 17/802,607, filed on Aug. 26, 2022, filed as application No. PCT/US21/20335 on Mar. 1, 2021, now Pat. No. 12,313,549.

(60) Provisional application No. 62/982,463, filed on Feb. 27, 2020.

Publication Classification

(51) **Int. Cl.**
G01N 21/64 (2006.01)
G02B 21/00 (2006.01)

(52) **U.S. Cl.**
CPC ***G01N 21/6458*** (2013.01); ***G01N 21/6408*** (2013.01); ***G01N 21/6428*** (2013.01); ***G02B 21/002*** (2013.01); ***G02B 21/0076*** (2013.01)

(57) **ABSTRACT**

The present disclosure pertains to two-photon microscopy, and specifically to methods and systems for optimizing the performance of entangled two-photon absorption (ETPA) microscopy. An ETPA microscope is described with time delay tunability to optimize the coincidence of entangled photons on a sample. The optimization allows for increased two-photon absorption by the sample, resulting in increased luminescence of the sample. The ETPA microscopy systems and methods described allow for nonlinear imaging using excitation energy intensities six orders of magnitude lower than comparable two-photon absorption microscopy techniques using classical light.

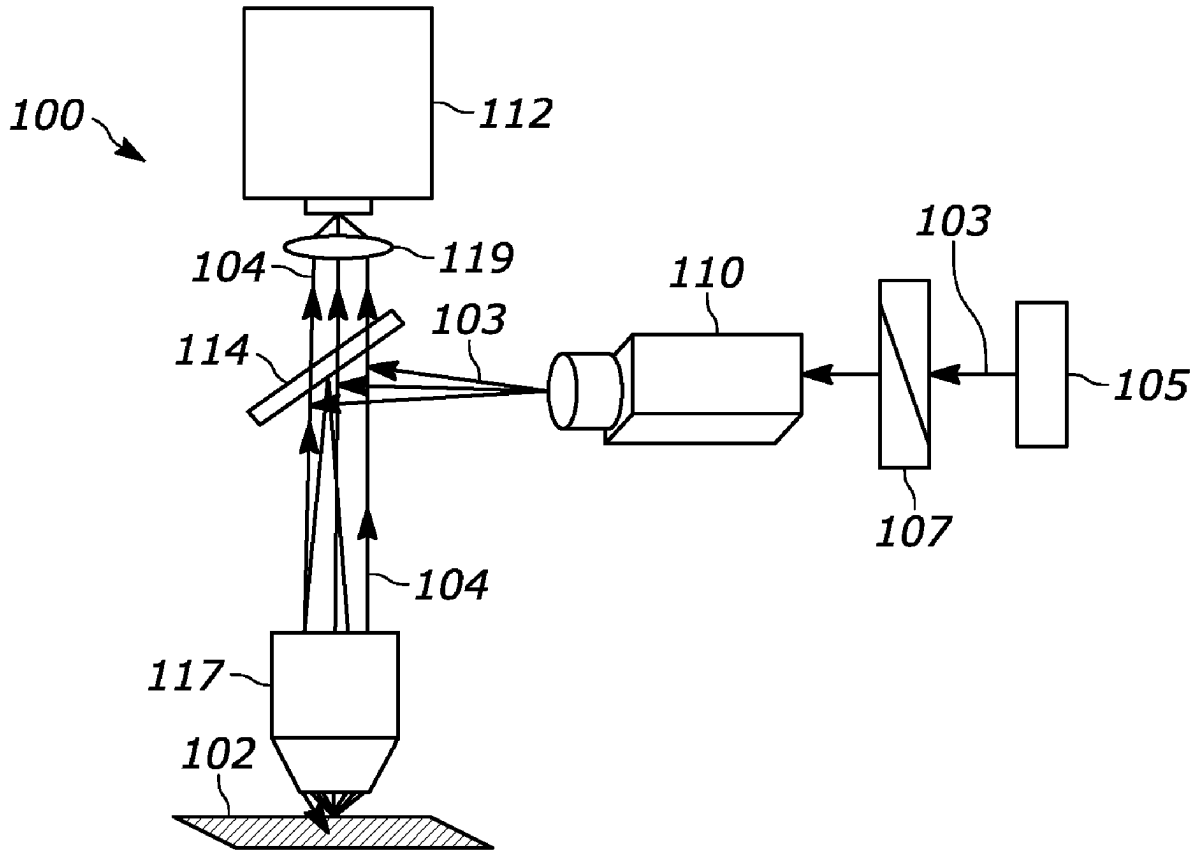

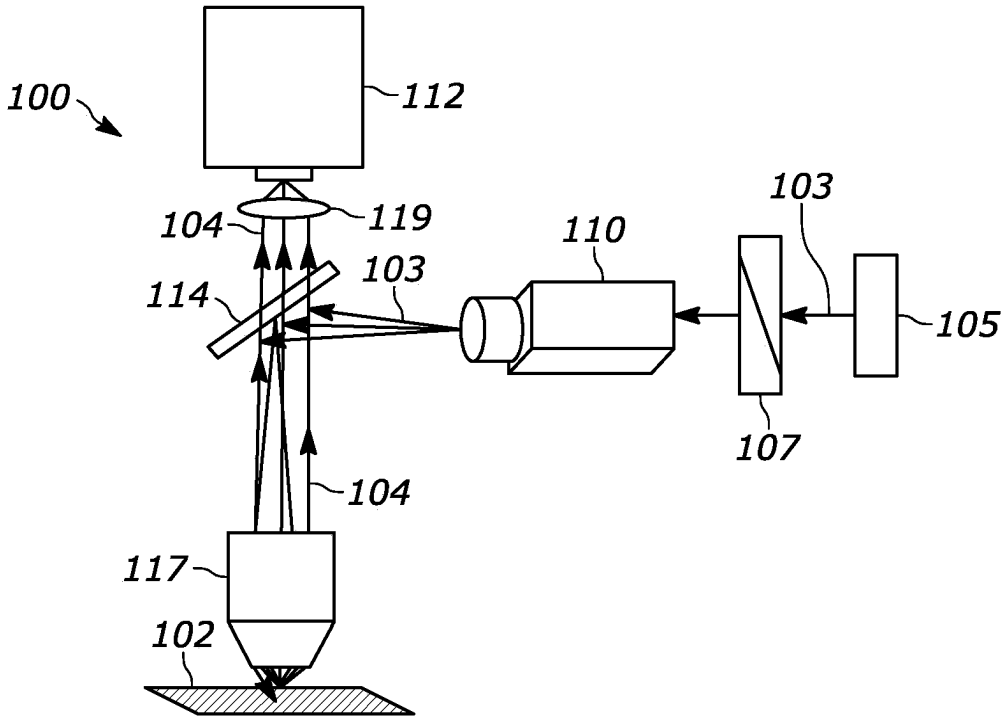
100
112
104
119
110
103
114
103
105
107
104
117
102

FIG. 1

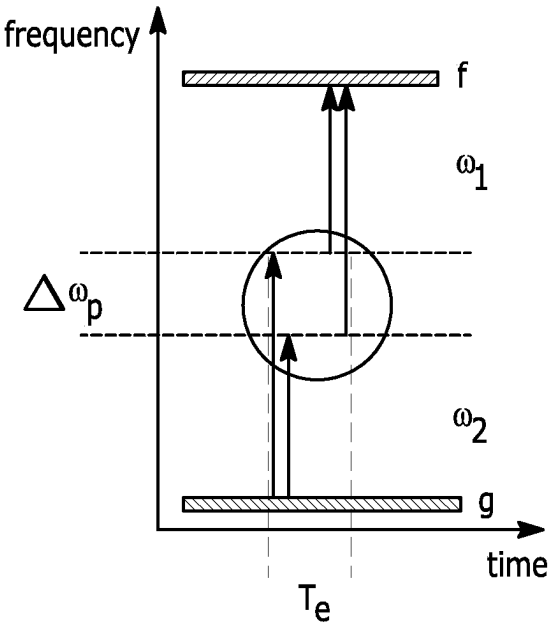
frequency
f
ω1
Δωp
ω2
g
time
Te

FIG. 2

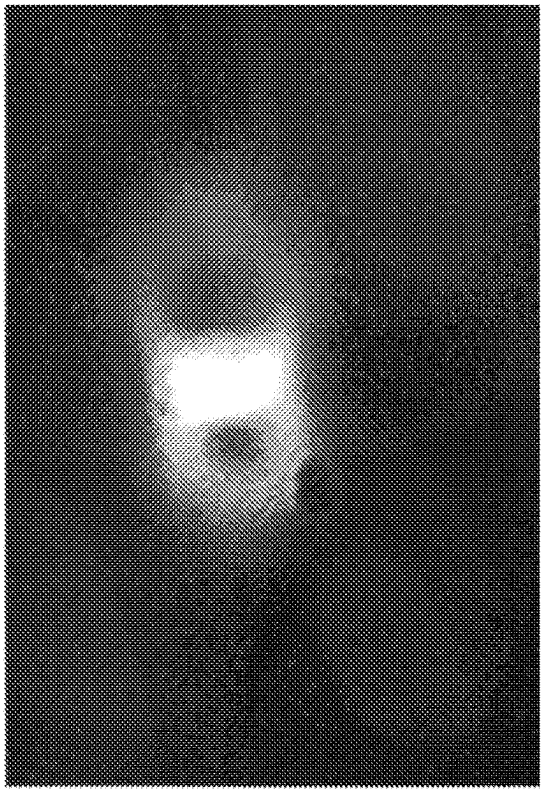

FIG. 3B

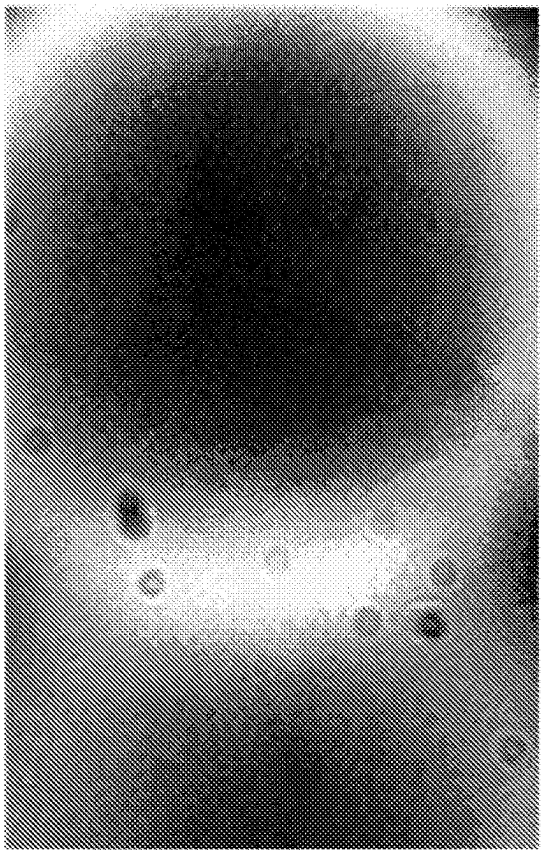

FIG. 3A

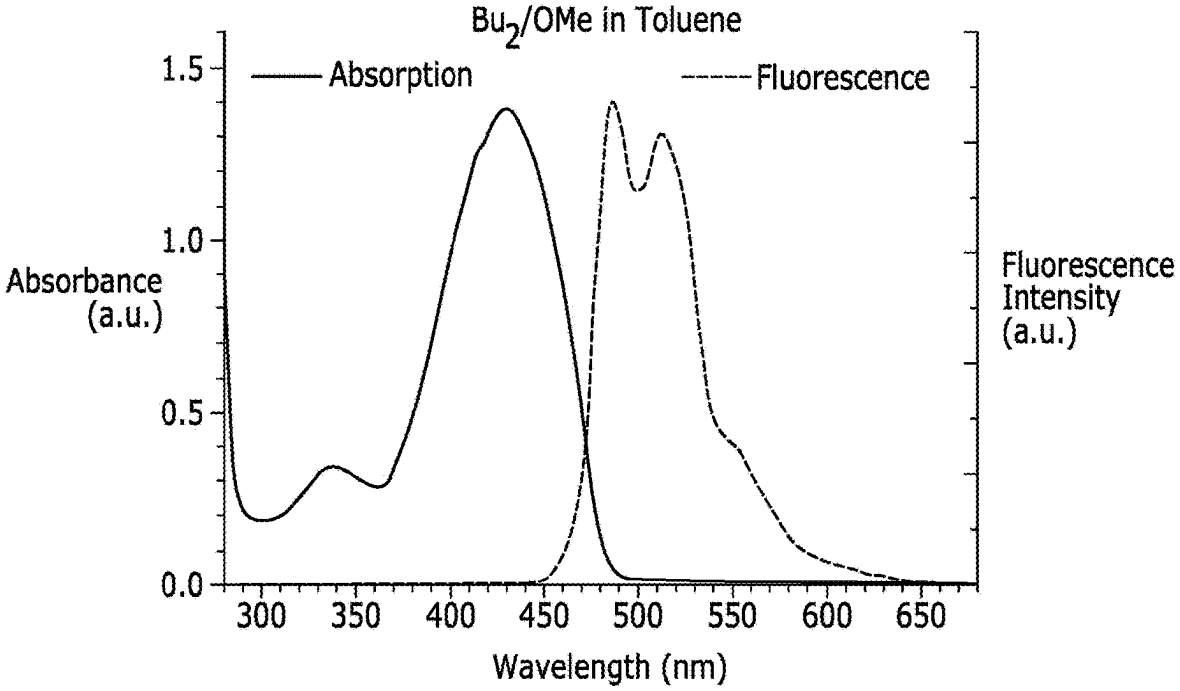
Bu2/OMe in Toluene
Absorption
Fluorescence
1.5
1.0
0.5
0.0
Absorbance (a.u.)
Fluorescence Intensity (a.u.)
300
350
400
450
500
550
600
650
Wavelength (nm)

FIG. 4

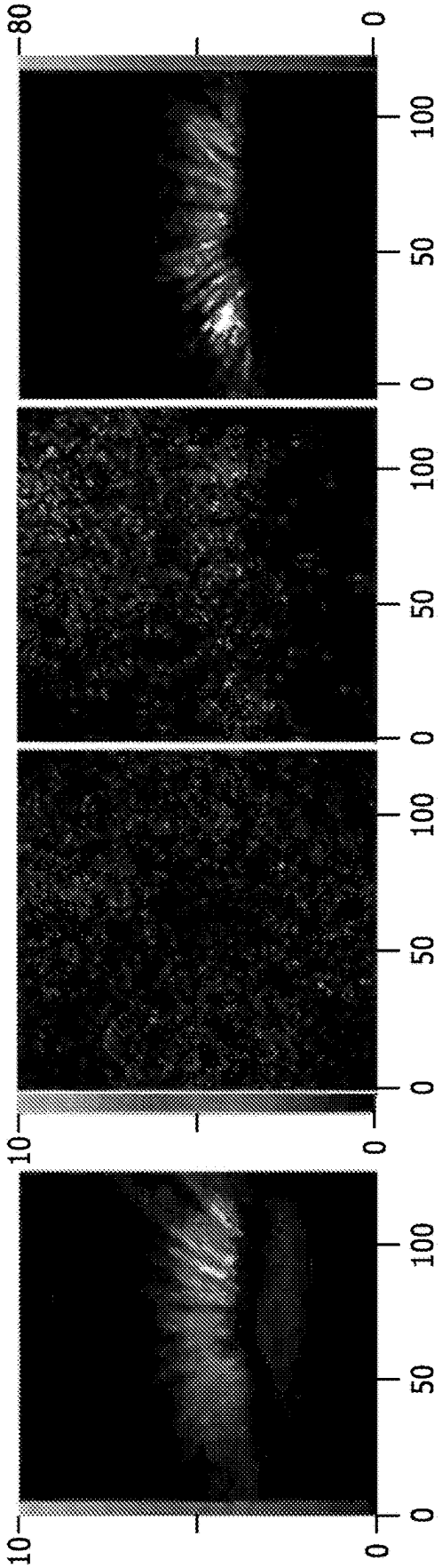

FIG. 5D

FIG. 5C

FIG. 5B

FIG. 5A

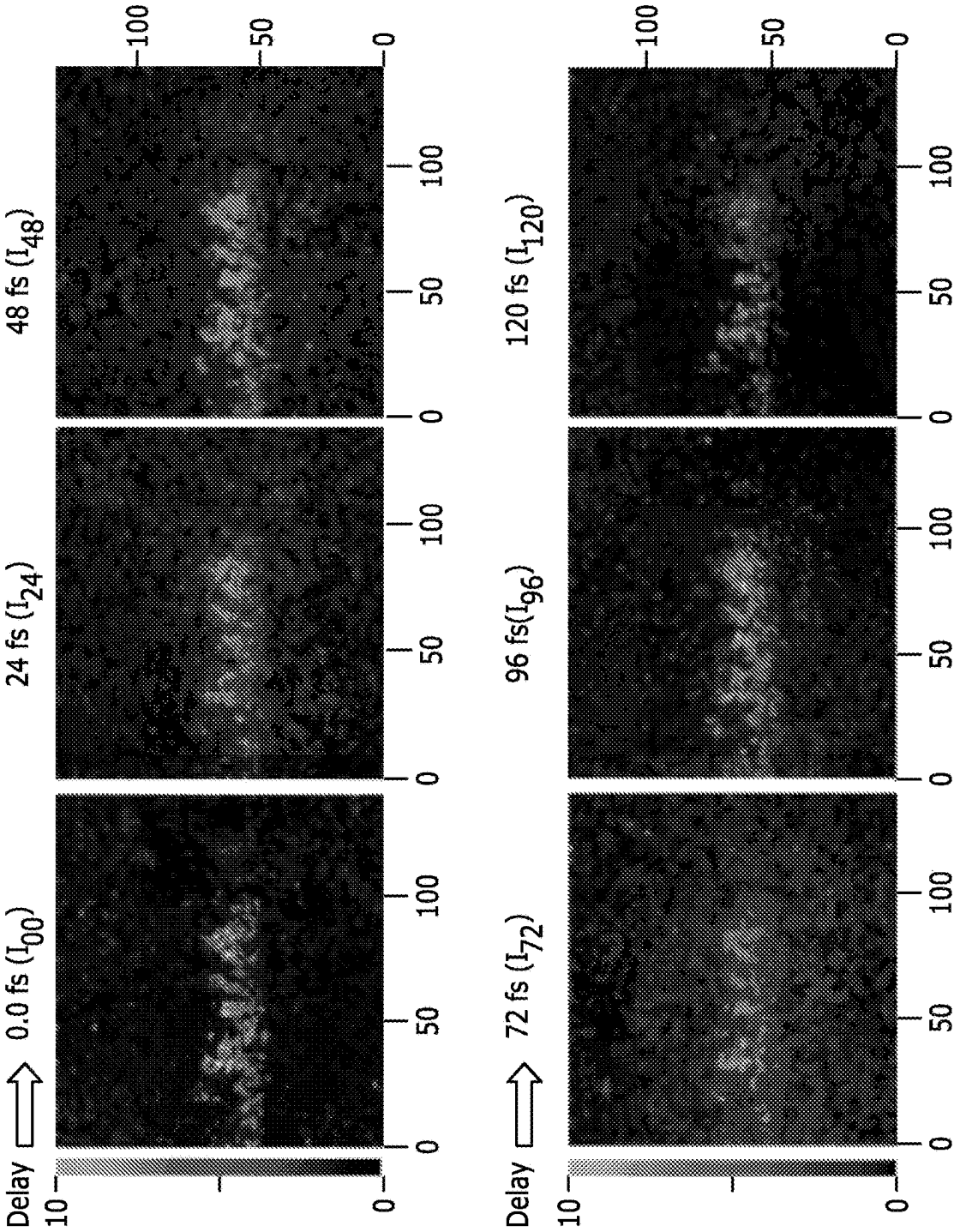
Delay
10
0
0.0 fs (I_{00})
24 fs (I_{24})
48 fs (I_{48})
72 fs (I_{72})
96 fs(I_{96})
120 fs (I_{120})
0
50
100

FIG. 6

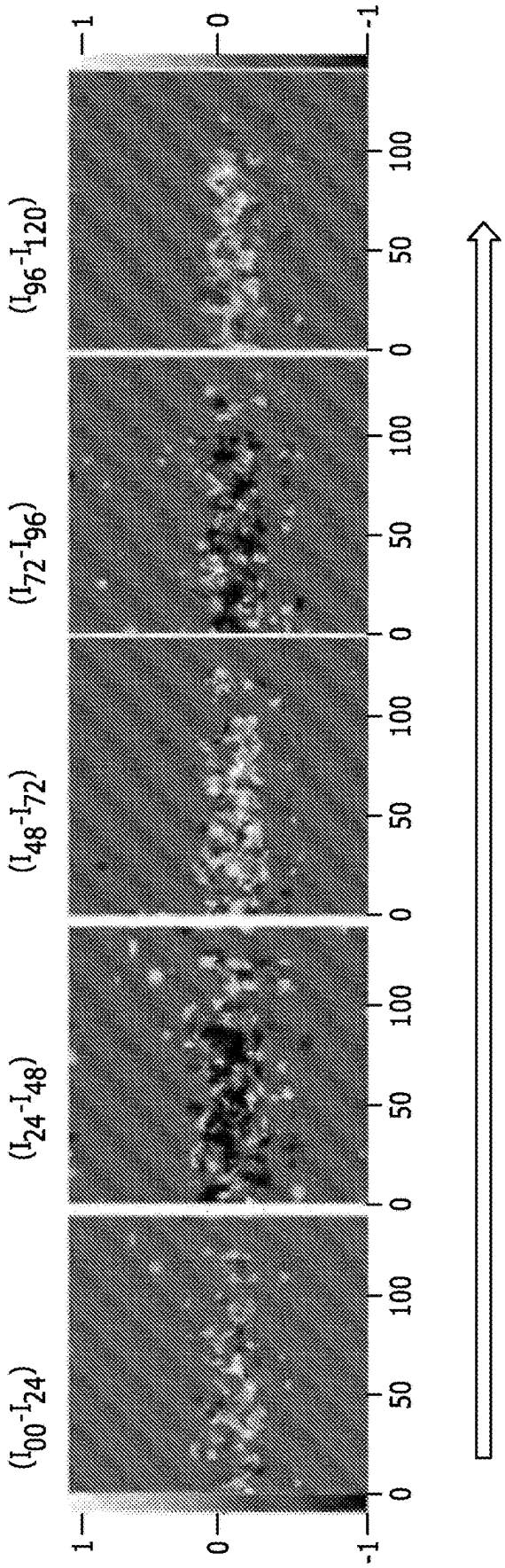

FIG. 7

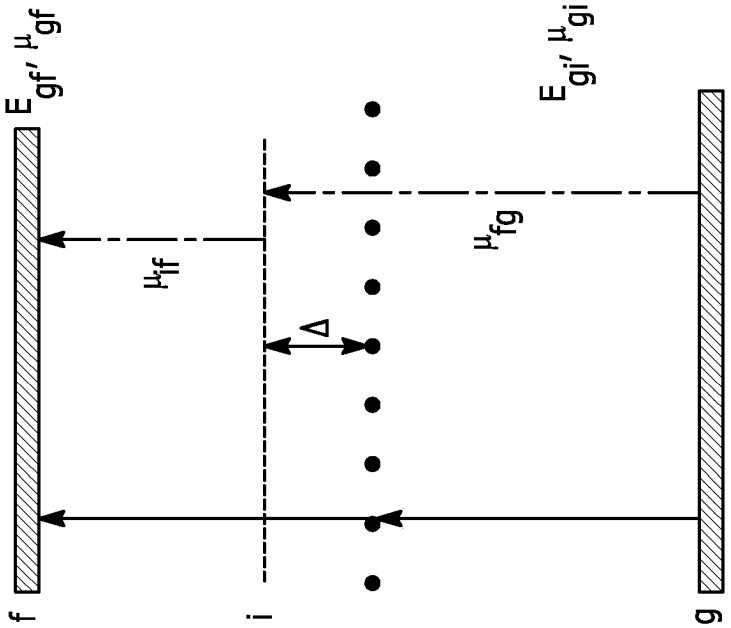

FIG. 8B

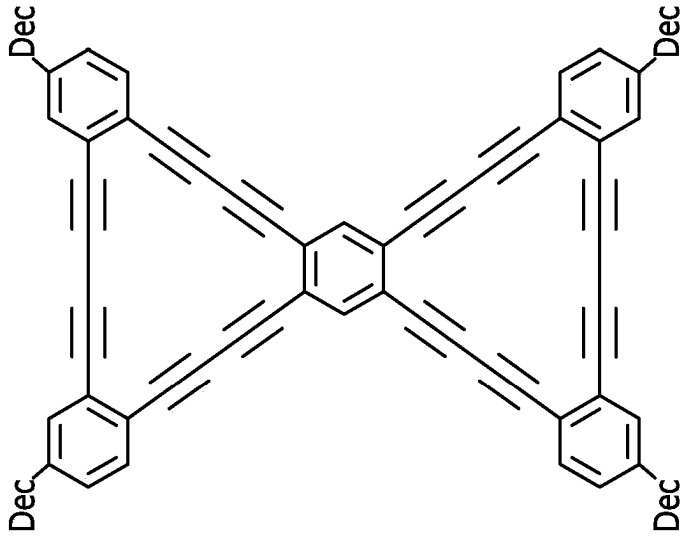

FIG. 8A

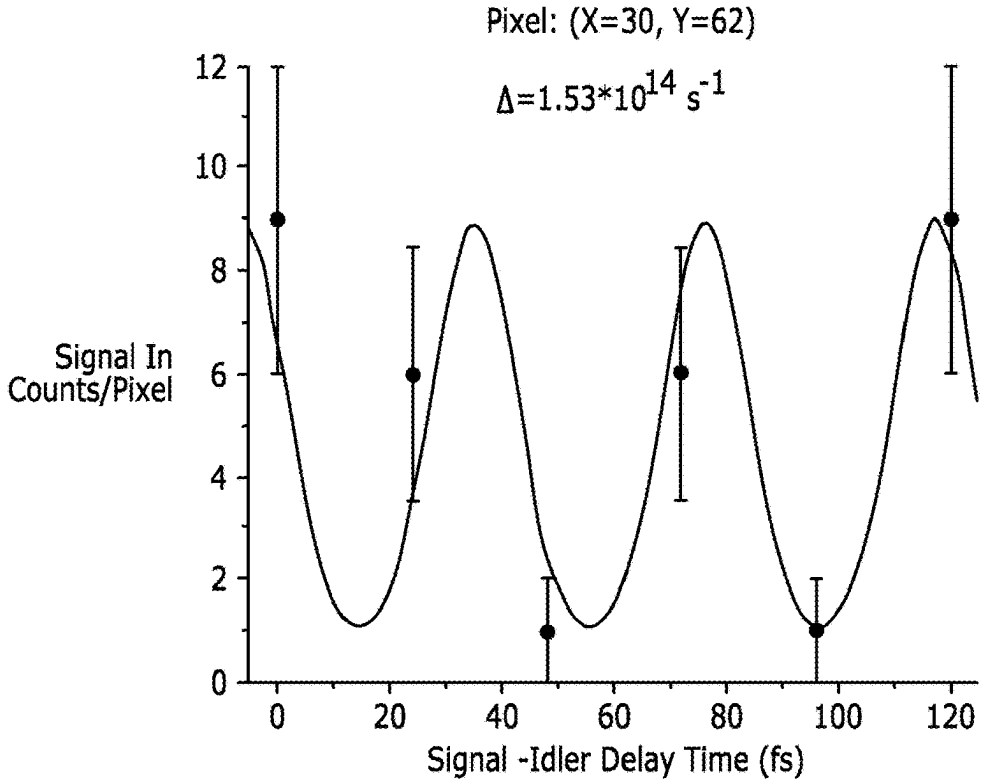
Pixel: (X=30, Y=62)
Δ=1.53*10^14 s^-1
Signal In Counts/Pixel
0
2
4
6
8
10
12
0
20
40
60
80
100
120
Signal -Idler Delay Time (fs)

FIG. 9A

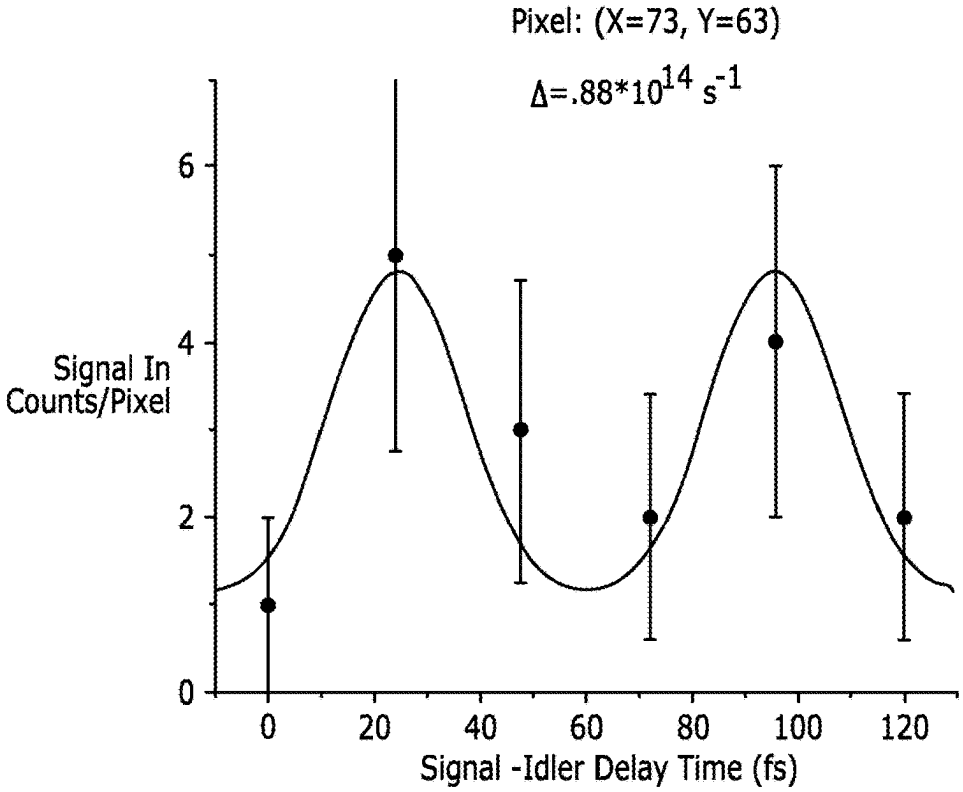
Pixel: (X=73, Y=63)
Δ=.88*10^14 s^-1
Signal In Counts/Pixel
0
2
4
6
0
20
40
60
80
100
120
Signal -Idler Delay Time (fs)

FIG. 9B

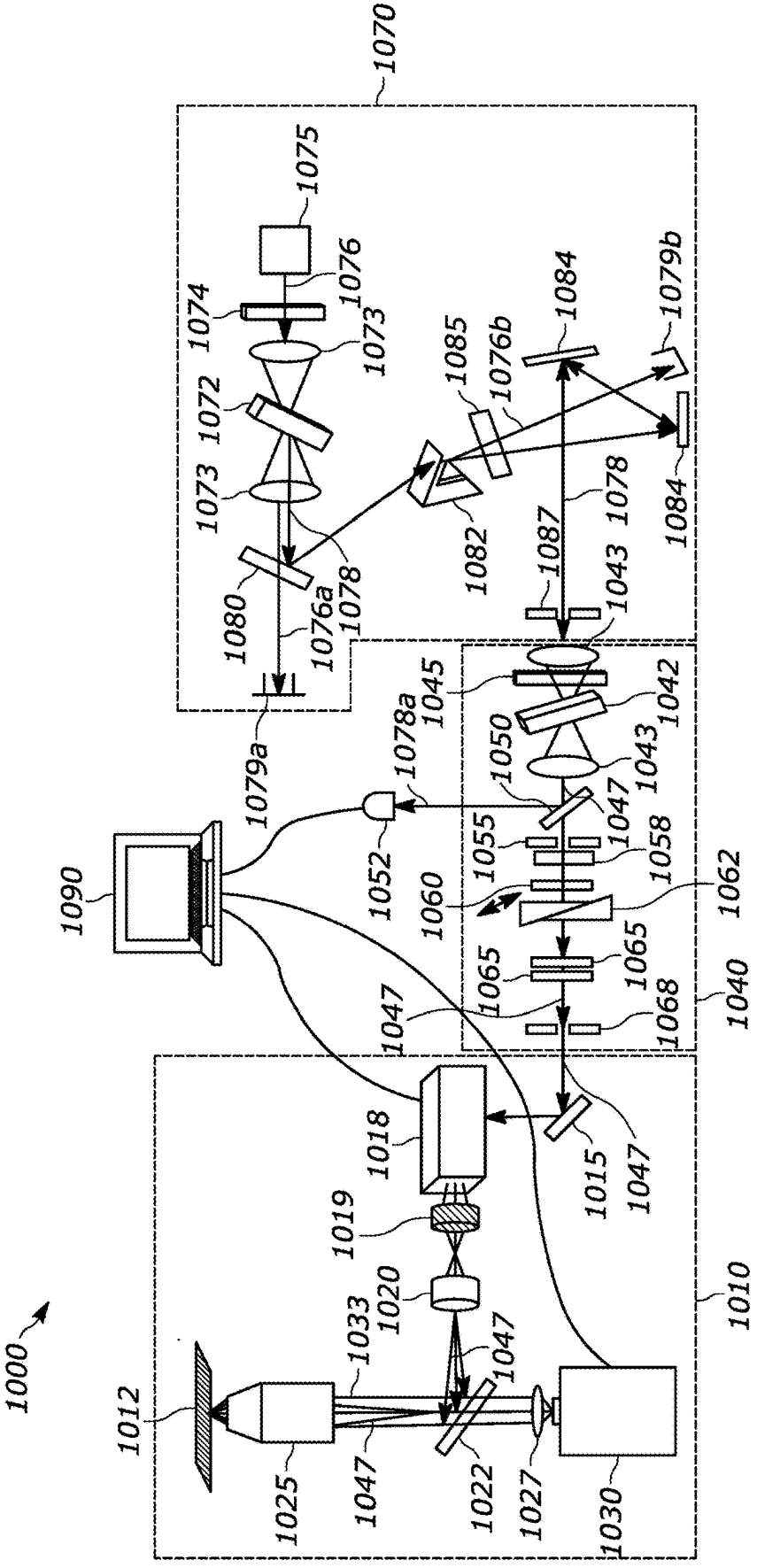
1000
1010
1012
1018
1019
1020
1022
1025
1027
1030
1033
1040
1042
1043
1045
1047
1050
1052
1055
1058
1060
1062
1065
1068
1070
1072
1073
1074
1075
1076
1076a
1076b
1078
1078a
1079a
1079b
1080
1082
1084
1085
1087
1090

FIG. 10

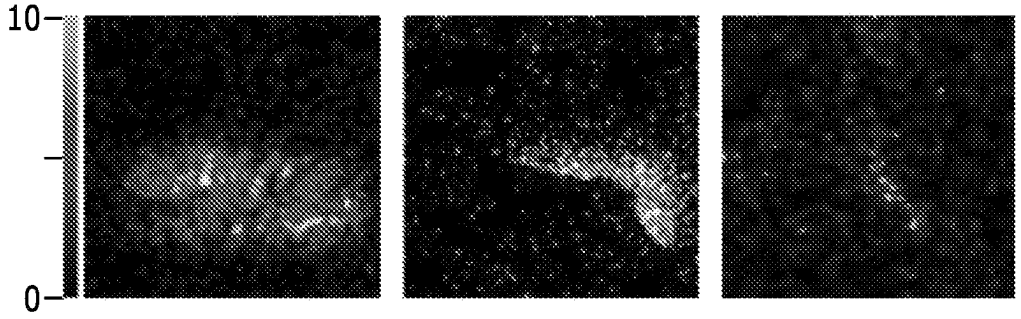

FIG. 11A FIG. 11D FIG. 11G

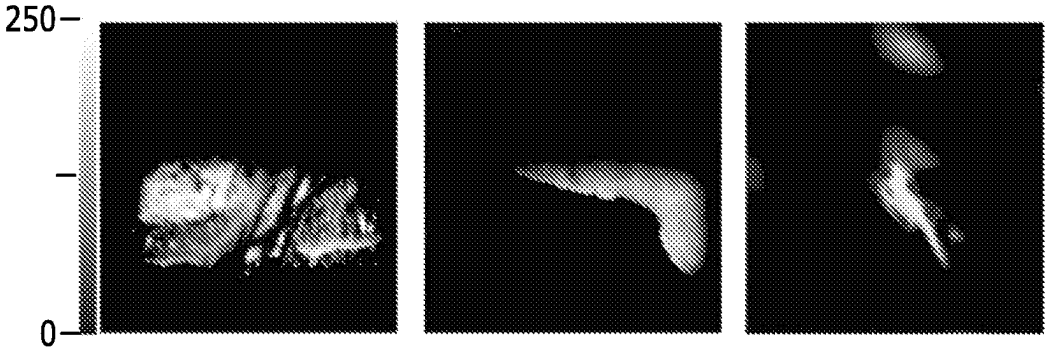

FIG. 11B FIG. 11E FIG. 11H

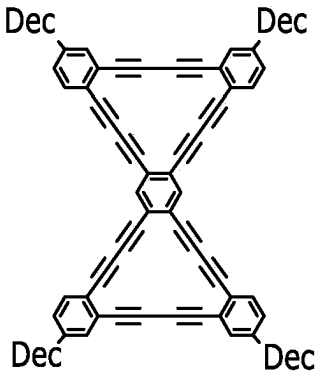

Bis[18]Annulene BT

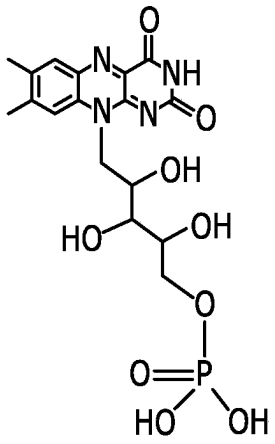

Flavin Mononucleotide (FMN)

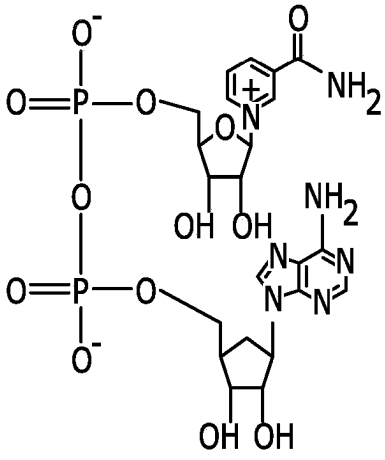

Nicotinamide Adenine Dinucleotide (NADH)

FIG. 11C FIG. 11F FIG. 11I

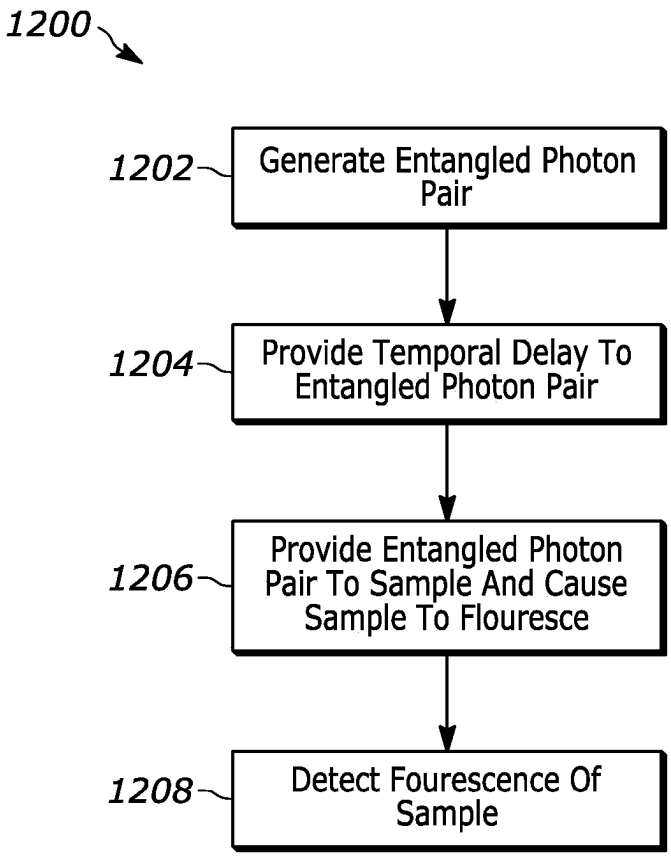
1200
1202
Generate Entangled Photon Pair
1204
Provide Temporal Delay To Entangled Photon Pair
1206
Provide Entangled Photon Pair To Sample And Cause Sample To Flouresce
1208
Detect Fourescence Of Sample

FIG. 12

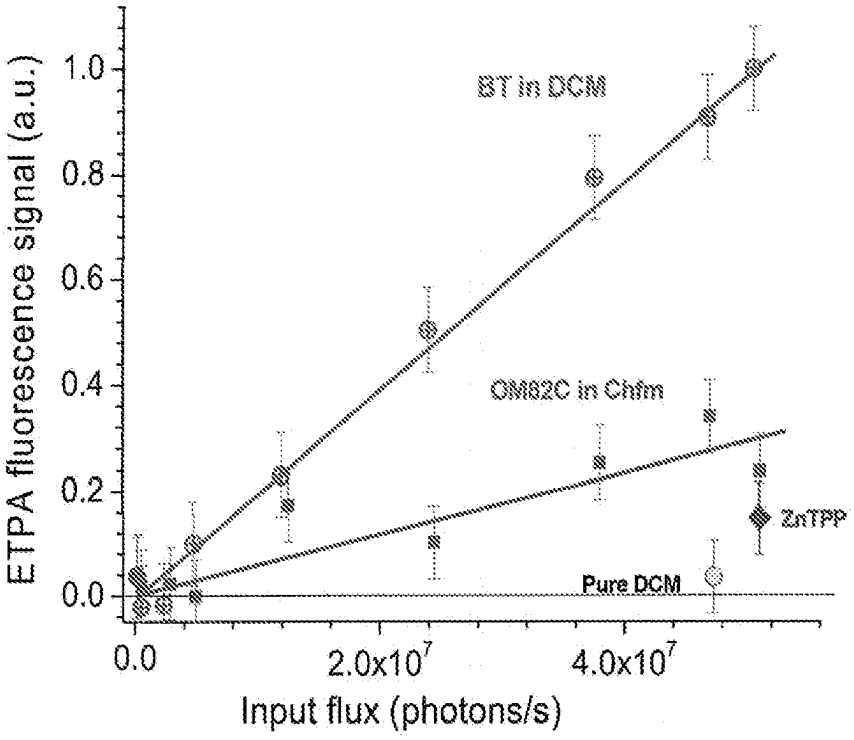
ETPA fluorescence signal (a.u.)
1.0
0.8
0.6
0.4
0.2
0.0
ST in DCM
OM82C in Chfm
ZnTPP
Pure DCM
0.0
2.0x10^7
4.0x10^7
Input flux (photons/s)

FIG. 13

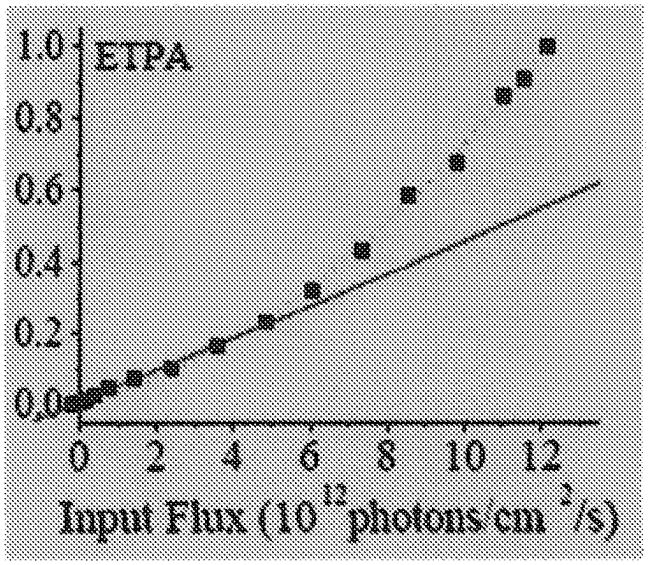

FIG. 14A

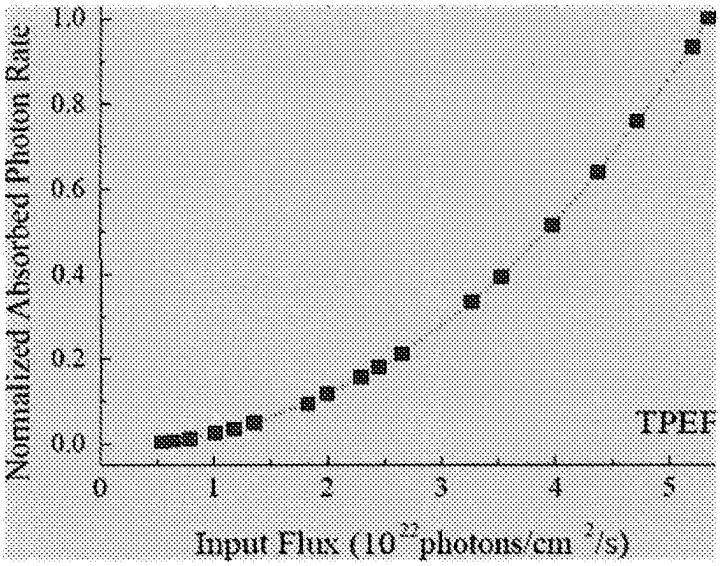

FIG. 14B

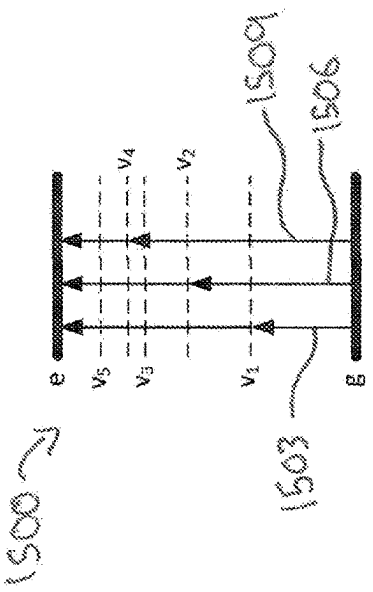

FIG. 15

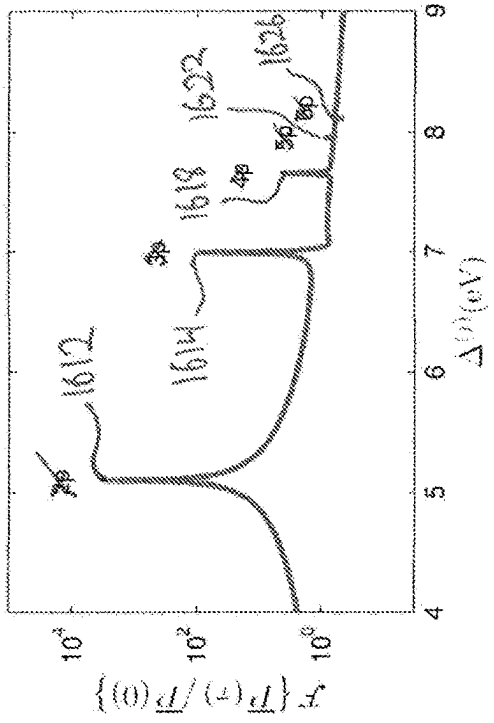

FIG. 16B

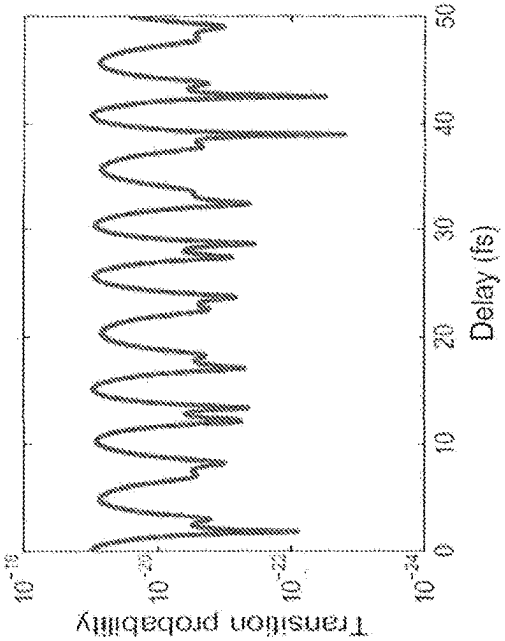

FIG. 16A

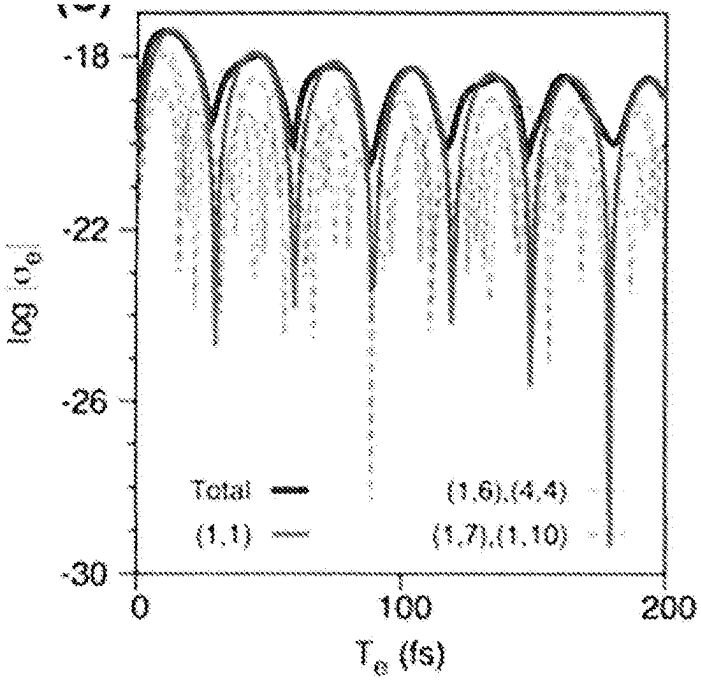

FIG. 17A

	experiment	theory			
molecule	σ_e (10^{-19} cm^2)	f	σ_e (10^{-19} cm^2)	g_e (μs)	$\gamma_{//}/\gamma_\perp$
6T (planar)	1.3	ES2	1.7	988	6×10^{-4}
6T (twisted)		ES2	0.18	178	3×10^{-3}
18T	7.1	ES2	5.3	853	6×10^{-4}
		ES3	1.2	84	6×10^{-3}

FIG. 17B

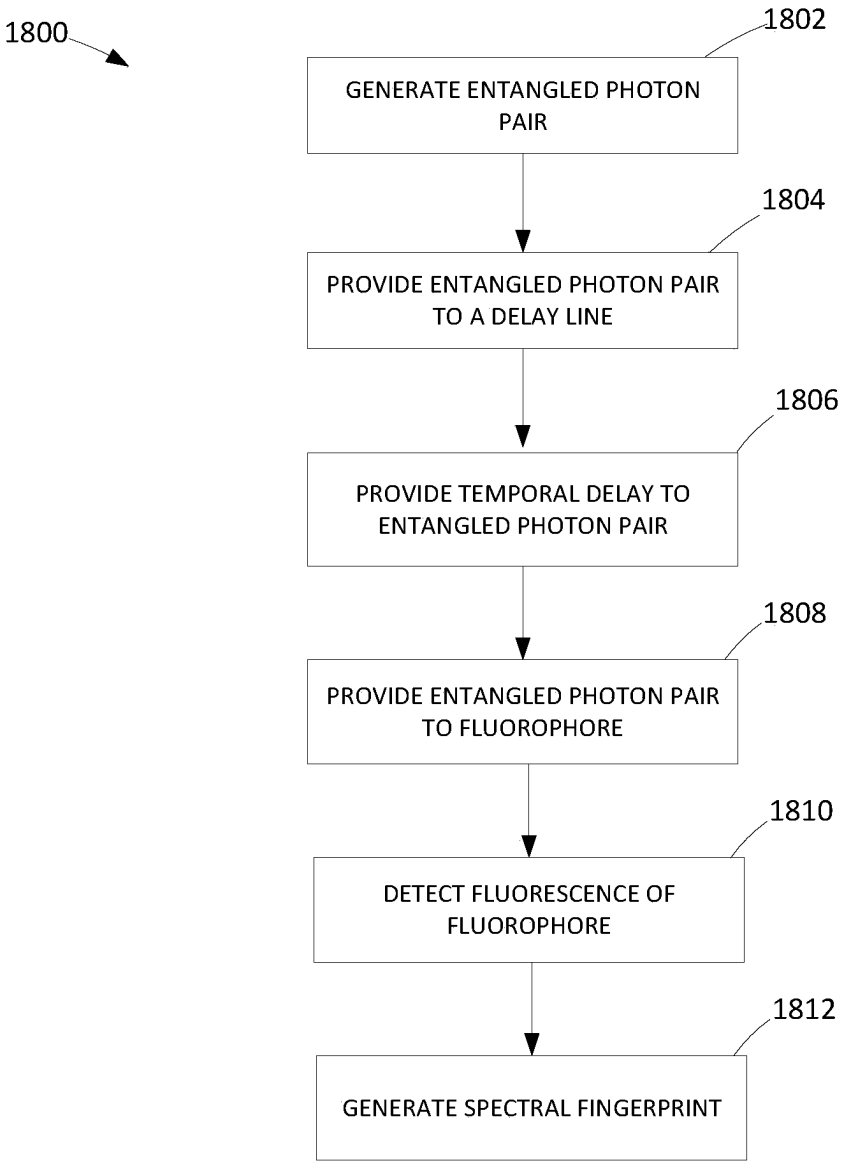
1800
1802
GENERATE ENTANGLED PHOTON PAIR
1804
PROVIDE ENTANGLED PHOTON PAIR TO A DELAY LINE
1806
PROVIDE TEMPORAL DELAY TO ENTANGLED PHOTON PAIR
1808
PROVIDE ENTANGLED PHOTON PAIR TO FLUOROPHORE
1810
DETECT FLUORESCENCE OF FLUOROPHORE
1812
GENERATE SPECTRAL FINGERPRINT

FIG. 18

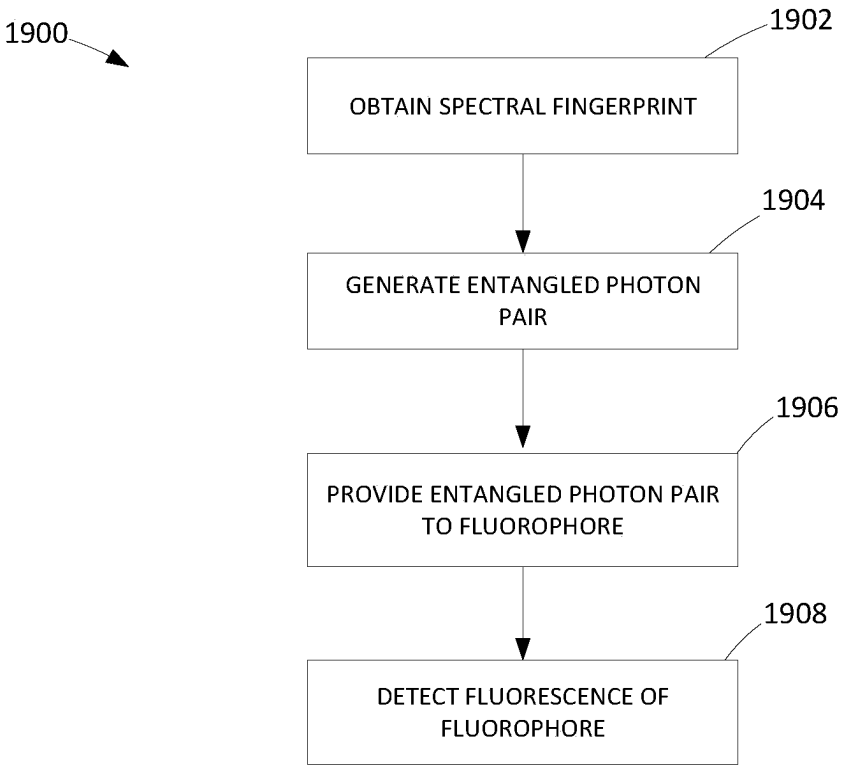
1900
1902
OBTAIN SPECTRAL FINGERPRINT
1904
GENERATE ENTANGLED PHOTON PAIR
1906
PROVIDE ENTANGLED PHOTON PAIR TO FLUOROPHORE
1908
DETECT FLUORESCENCE OF FLUOROPHORE

FIG. 19

TWO-PHOTON FLUORESCENCE MICROSCOPY AT EXTREMELY LOW EXCITATION INTENSITY

CROSS-REFERENCE TO RELATED APPLICATION

[0001] Priority is claimed to U.S. Provisional Patent Application No. 62/982,463, filed Feb. 27, 2020, the entire disclosure of which is incorporated herein by reference.

STATEMENT OF GOVERNMENT SUPPORT

[0002] This invention was made with government support under CHE1607949 awarded by the National Science Foundation. The government has certain rights in the invention.

FIELD OF THE INVENTION

[0003] The disclosure relates generally to methods and systems for performing microscopy, and specifically to two-photon microscopy systems.

BACKGROUND

[0004] The background description provided herein is for the purpose of generally presenting the context of the disclosure. Work of the presently named inventor, to the extent it is described in this background section, as well as aspects of the description that may not otherwise qualify as prior art at the time of filing, are neither expressly nor impliedly admitted as prior art against the present disclosure.

[0005] Fluorescent microscopy is a microscopy imaging method that uses fluorescence to study the properties of organic or inorganic targets. Typically, a target for imaging is illuminated by light having a specific wavelength which is absorbed by fluorophores. The fluorophores then emit light having a wavelength longer than that of the illuminating light. Spectral filtering is then applied to separate the fluorescent light from the illumination light for imaging of the target.

[0006] Over time, fluorophores lose the ability to fluoresce as they are illuminated by a process called photobleaching. Photobleaching occurs over time as fluorescent molecules accumulate chemical damage from electrons that are excited during the fluorescent process. Further, living cells and target samples may be damaged by intense illumination light required for performing fluorescent, or fluorophores may generate reactive chemical species which leads to phototoxicity effects.

[0007] Two-photon excitation fluorescence (TPEF) microscopy is a technique that utilizes the nonlinear effect of two-photon absorption for performing fluorescent microscopy imaging. TPEF microscopy requires excitation of a fluorophore by two photons simultaneously. Typical TPEF utilizes near-infrared illumination light which reduces scattering in samples, compared to other fluorescent microscopy techniques. Also, due to multiphoton absorption, background signals are very weak increasing image resolution and contrast. Further, the use of two-photon absorption reduces the effects of photobleaching and allows for deeper penetration depths.

[0008] Two-photon absorption must occur with two-photons simultaneously, and therefore, it is much weaker and less likely to occur as compared to single-photon absorption. To increase the rates of two-photon absorption high intensities of illumination light are required which can destroy tissues, cells, other living targets, or disrupt molecular and electrical bonds. Moreover, the signal-to-noise ratio (SNR) for a given light intensity is limited by the standard quantum limit, which is often important for the measurements where the probe light intensity is reduced to avoid damaging the sample. Further, the standard quantum limit also limits the spatial resolution of TPEF microscopy images.

[0009] Thus, there is a need for a method for performing high resolution fluorescent imaging of samples that utilizes low intensity illumination light to avoid damaging the sample. Additionally, there is need for microscopy methods that are not limited by the standard quantum limit, for high spatial resolution of targets at the sub-micron scale.

SUMMARY OF THE INVENTION

[0010] In example embodiments, ETPA microscopy system and methods include signal-idler delay scanning enabling the selectivity of excitations of particular states/species in a sample, and further including performing local specimen spectroscopy. Other example embodiments include methods that include spontaneous parametric down conversion (SPDC)-microscope coupling enhancements utilizing entangled photon beam characterization and optimization of the entangled photon scanner throughput at the microscope objective lens. Yet other example embodiments include a light-tight microscope enclosure allowing quick sample change and dark count rate below 1 photon/pixel. In other example embodiments, methods and systems include signal collecting and processing procedures that utilize a time-gated photon counter synchronized with the microscope scanner to provide a high signal-to noise ratio.

BRIEF DESCRIPTION OF THE DRAWINGS

[0011] The figures described below depict various aspects of the system and methods disclosed herein. It should be understood that each figure depicts an embodiment of a particular aspect of the disclosed system and methods, and that each of the figures is intended to accord with a possible embodiment thereof. Further, wherever possible, the following description refers to the reference numerals included in the following figures, in which features depicted in multiple figures are designated with consistent reference numerals.

[0012] FIG. **1** is a block diagram of an example microscopy system for performing entangled two-photon absorption (ETPA) microscopy, in accordance with an example.

[0013] FIG. **2** is a diagram of a frequency time plot illustrating the entanglement time of entangled photon pairs generated by spontaneous parametric down conversion (SPDC), in accordance with an example.

[0014] FIG. **3**A is an image of the output transverse beam profile characteristic for a type-II SPDC configuration as captured by a charged coupled device (CCD) camera installed at an output port of an entangled photon source, in accordance with an example.

[0015] FIG. **3**B is an image captured by a CCD camera at the output port of an entangled photon source with a maximally overlapped collimated SPDC beam, in accordance with an example.

[0016] FIG. **4** is a plot showing absorbance and fluorescent intensity as a function of wavelength of bis-(styryl) benzene derivative Bu_2/OMe as obtained by an ETPA microscopy system, in accordance with an example.

[0017] FIG. **5**A is an image of Bu_2/OMe in a drop cast film generated by the ETPA microscopy system of FIG. **1** with an excitation flux of 10^7 photons/s, in accordance with an example.

[0018] FIG. **5**B is an image of Bu_2/OMe in a drop cast film captured by a classical light two-photon absorption (TPA) microscopy system with an excitation flux of 0.96×10^{12} photons/s, in accordance with an example.

[0019] FIG. **5**C is an image of Bu_2/OMe in a drop cast film captured by a classical light TPA microscopy system with an excitation flux of 0.96×10^{13} photons/s, in accordance with an example.

[0020] FIG. **5**D is an image of Bu_2/OMe in a drop cast film captured by a classical light TPA microscopy system with an excitation flux of 5×10^{13} photons/s, in accordance with an example.

[0021] FIG. **6** presents a series of images of microcrystalline aggregates of bis[18]-annulene in a cast film at different signal-idler delays as obtained by the ETPA microscopy system of FIG. **1**, in accordance with an example.

[0022] FIG.**7** presents a set of differential images constructed by subtracting the image $I_{\tau i}$ obtained with time delay τ_i from an image $I_{\tau k}$ obtained with a time delay τ_k with k−i=1, in accordance with an example.

[0023] FIG. **8**A is a diagram of a biz[18]annulene (BT) molecule used in the ETPA imaging, in accordance with an example.

[0024] FIG. **8**B is an energy band diagram of a BT molecule assuming a single dominant intermediate level in a two-photon transition, in accordance with an example.

[0025] FIG. **9**A is a plot of signal counts per pixel and a fit of theoretical fluorescence dependence on signal-idler delay at a first pixel location, in accordance with an example.

[0026] FIG. **9**B is a plot of signal counts per pixel and a fit of theoretical fluorescence dependence on signal-idler delay at a second pixel location different than the pixel location of FIG. **9**A, in accordance with an example.

[0027] FIG. **10** is a diagram of another example system for performing ETPA microscopy, in accordance with an example.

[0028] FIG. **11**A is an ETPA microscopy image of a biz[18]annulene (BT) drop cast film, in accordance with an example.

[0029] FIG. **11**B is a classical TPA microscopy image of a BT drop cast film, in accordance with an example.

[0030] FIG. **11**C is a diagram of the molecular structure of BT.

[0031] FIG. **11**D is an ETPA microscopy image of a flavin mononucleotide (FMN) drop cast film, in accordance with an example.

[0032] FIG. **11**E is an classical TPA microscopy image of a FMN cast film, in accordance with an example.

[0033] FIG. **11**F is a diagram of the molecular structure of FMN.

[0034] FIG. **11**G is an ETPA microscopy image of an anicotinamide adenine dinucleotide (NADH) drop cast film, in accordance with an example.

[0035] FIG. **11**H is an classical TPA microscopy image of a NADH drop cast film, in accordance with an example.

[0036] FIG. **11**I is a diagram of the molecular structure of NADH.

[0037] FIG. **12** is a flow diagram of a method for performing ETPA microscopy, in accordance with an example.

[0038] FIG. **13** is a plot of ETPA fluorescence versus input flux of excitation entangled photon pair beams for three different fluorophores, in accordance with an example.

[0039] FIG. **14**A is a plot of normalized absorbed photon rate versus input flux for ETPA of an organic molecule, in accordance with an example.

[0040] FIG. **14**B is a plot of normalized absorbed photon ate versus input flux for classical TPA, in accordance with an example.

[0041] FIG. **15** is an example energy band diagram of a molecule having a ground energy state, g, an excited energy state, e, and multiple virtual energy states, v_1 through v_5, in accordance with an example.

[0042] FIG. **16**A is a plot of simulated excitation transition probability of a hydrogen molecule versus signal-idler delay of an SPDC bi-photon pair, in accordance with an example.

[0043] FIG. **16**B is a plot of the Fourier transform of the time delay plot of FIG. **16**A, in accordance with an example.

[0044] FIG. **17**A is a plot of entanglement cross section versus entanglement time, T_e, for ETPA in a thiophene dendrimer, in accordance with an example.

[0045] FIG. **17**B presents a table of the measured experimental entanglement cross-section values determined from the data illustrated in the plot of FIG. **17**A, and the theoretically determined entanglement cross-section values for an entangled photon pair in the thiophene dendrimer, in accordance with an example.

[0046] FIG. **18** is a flow diagram of a method for determining a fingerprint of a molecule using ETPA spectroscopy, in accordance with an example.

[0047] FIG. **19** is a flow diagram of a method for using a fluorophore fingerprint to perform microscopy or spectroscopy of a fluorophore, in accordance with an example.

DETAILED DESCRIPTION

[0048] Quantum entanglement has been shown to imply correlations stronger than those allowed by classical models. The possibility of performing tasks which are classically impossible has made quantum entanglement a powerful resource for the development of novel methods and applications in various fields of research such as quantum computing, quantum cryptography, and quantum metrology. Applications of non-classical light to molecular spectroscopy have recently received increasing attention offering novel powerful spectroscopic tools. There is a great need for the development of next generation spectroscopic instrumentation and technologies utilizing entangled quantum light. Among the many applications of non-classical states of light, nonlinear microscopy has the potential to make an impact in broad areas of science from physics to biology.

[0049] Entangled two-photon microscopy offers nonlinear imaging capabilities at a low excitation intensity which is six orders of magnitude lower than the excitation level required for classical two-photon image. The disclosed methods and systems enable capturing of microscopic images created by fluorescence selectively excited by the process of entangled two-photon absorption. The obtained images depend on a femtosecond scale delay between components of the entangled photon pair. The delay dependence is a result of specific quantum interference effects associated with the entanglement which is not observable using classical excitation light. In combination with novel spectroscopic capabilities provided by a non-classical light excitation, the

disclosed imaging systems and methods are importance for sensing and biological applications, among others.

[0050] Utilizing non-classical states of light possessing highly correlated photons enables low-intensity imaging and microscopy, and more precise measurements, at intensities not achievable with classical resources. The described systems and methods are not limited by the standard quantum limit (SQL) which allows for increased spatial resolution as compared to other two-photon imaging techniques. The two-photon fluorescent microscopy methods and systems described herein utilize the entangled two-photon absorption (ETPA) effect to induce the fluorescence of the sample in the microscope. Due to energy-time entanglement the absorption of entangled photon pairs can be very efficient at low power in comparison with classical random two-photon absorption enabling extremely low intensity microscopic measurements. Qualitatively, both components of the entangled photon pair arrive at the same location almost simultaneously, thereby providing an enhanced two-photon absorption efficiency and subsequent and fluorescence efficiency. The two-photon absorption enhancement allows for the excitation light intensity much lower than that required for classical light TPA for a same fluorescence intensity. To further reduce the excitation intensity, the described systems and methods may provide enhanced spatial resolution from the entanglement of signal and idler by the same mechanism as in quantum lithography with a two-beam excitation beam geometry.

[0051] ETPA efficiency exhibits a non-monotonic dependence on a time delay between entangled pair components. The non-monotonic behavior is a unique property of the non-classical light of ETPA. The period profile of the non-monotonic dependence on the inter-component delay contains the spectroscopic signature of a target material and can be used as a powerful spectroscopic tool to determine components of a material. Therefore, the quantum interference of ETPA can be used to characterize a material system with which the entangled photon pair is interacting. The described methods and systems utilize the non-monotonic ETPA efficiency by providing a tunable signal-idler time delay to perform ETPA microscopy and spectroscopy.

[0052] FIG. **1** is a diagram of an embodiment of a microscopy system **100** for perform ETPA microscopy. The system **100** includes a sample **102**, an entangled photon source **105**, a delay line **107**, a scanner **110**, and a detector **112**. The entangled photon source **102** generates an entangled photon pair **103** that propagates along an axis of propagation. The entangled photon pair **103** includes an idler photon and a signal photon. The delay line **107** is disposed along the axis of propagation and is configured to provide a temporal delay between the idler and the signal photons of the photon pair **103**. Thus the delay line is an example of a temporal delay line that is formed of one or more of a birefringent delay line, a freespace delay line, a fiber delay line, a dispersive delay line, or another type of optical delay line.

[0053] The scanner **110** changes the trajectory of the photon pair **103** to provide the photon pair **103** to different transverse locations of the sample **103** for imaging of the sample **103**. A dichroic beam splitter **114** directs the photon pair **103** toward an objective lens **117**, and the objective lens **117** focuses the photon pair **103** onto the sample **103**. The sample **103** absorbs the photon pair **103** and emits fluorescence **104**. The dichroic beam splitter **114** transmits the fluorescence **104** and a lens **119** focuses the fluorescence **104** onto the detector **112**. The detector **112** detects the fluorescence **104** and generates an electrical signal indicative of the detected fluorescence.

[0054] In an embodiments, the entangled photon source **105** generates the entangled photon pair **103** through spontaneous parametric down conversion (SPDC). FIG. **2** is a diagram of a frequency time plot illustrating the entanglement time of entangled photon pairs generated by SPDC. SPDC is a process by which a pump radiation having energy, $\hbar\omega_p$, with ω_p being a frequency of the radiation, excites an electron to an excited state and two photons having energies $\hbar\omega_1$ and $\hbar\omega_2$ are generated during de-excitation of the electron. Due to conservation of energy, $\omega_p=\omega_1+\omega_2$. Due to the pump radiation having a bandwidth, $\Delta\omega_p$, each of the energies ω_1 and ω_2 has an uncertainty that is dependent on the pump bandwidth. The circle in the middle of FIG. **2** illustrates the uncertainty due to the pump bandwidth, and how it may affect the uncertainties of the generated photon pair **103**. Further, due to the time-energy uncertainty principle, the entanglement time can be determined to be T_e, as illustrated in FIG. **2**. Therefore, SPDC generates a photon pair having an entanglement time T_e which can be further used to perform the ETPA microscopy as described herein.

[0055] An ETPA microscopy system was constructed according to the illustrated system **100** of FIG. **1**. The entangled photon source **105** generated the entangled photon pair **103** through SPDC in a BBO crystal. The SPDC in the BBO crystal was accomplished via type-II phase matching in the non-linear crystal. A source pump for the SPDC was provided by a femtosecond pump laser source. A Ti-sapphire laser (Mai Tai, Spectra Physics Inc.) supplied master pump radiation at a central wavelength of 800 nm with approximately a 7 nm bandwidth. The master pump radiation was converted to its second harmonic and the output pulse with the central wavelength 400 nm was directed towards the downconversion nonlinear crystal (i.e., the BBO crystal). A combination of a prism and an interference filter was used to separate the second harmonic from the fundamental. The BBO crystal was 1 mm thick and a two-photon quantum state was generated in the collinear configuration type-II SPDC in the BBO crystal. A dichroic mirror (DM) and an interference long pass filter (IF) with the cut on-wave wavelength at 750 nm (FEL0750, Thorlabs Inc.) were used to remove remaining 400 nm light. Insertion of a second filter FEL050 did not affect the count rates indicating no leak of the residual blue light. In some measurements and experiments an interference bandpass filter (IF) with the bandwidth 12 nm (FF01-800/12-25, Semrock Inc.) centered at 800 nm was used to select the near-degenerate biphotons. Each component of the entangled photon pair **103** (i.e., the signal photon and the idler photon) had a wavelength in the near-infrared range between 720 nm and 1500 nm. In examples, the entangled photon pair **103** may have a wavelength between 400 nm and 800 nm, between 600 nm and 1200 nm, between 1 micron and 5 microns, or another wavelength capable of being generated by SPDC. To evaluate the performance of the entangled photon source **105**, downconverted photons (i.e., entangled photon pairs) were detected by silicon avalanche photodiode (APD) single photon counting modules (Perkin-Elmer SPCM-AQR-13) or by a CCD camera (ST-402, SBIG Astronomical Instruments).

[0056] The entangled photon source **105** was able to produce $1.2*10^7$ photons/s output flux (singles). Diagnostics

of the SPDC output utilizing a polarizing beamsplitter and two APD detectors showed the signal-idler coincidence rate up to $1.5*10^6$ coincidence counts/s. Within type-II SPDC phase matching conditions, the signal (o-ray) and idler (e-ray) photons are generated at orthogonal polarizations. Polarization visibility measurements were been performed with a 50/50 non-polarizing beamsplitter and two polarizers placed in individual APD optical paths for both the signal and idler photons. The coincidence count rate as a function of the polarizer angle at one APD was collected. The measurement of the coincidence count rate showed a periodic modulation of the coincidence rate with a visibility of approximately 88.5%, while singles rates remained relatively constant. The visibility obtained is evidence of non-classical quantum interference given by polarization entangled states produced by SPDC.

[0057] The scanner **110** was a Galvo-Galvo Scan Head (4 mm input aperture diameter, LSK-GG, Thorlabs Inc.), and two scan lenses of 5 cm and 20 cm focal lengths (SL50-CLS2 and TL200-CLS2, respectively, Thorlabs Inc.) were used to scan an excitation beam angle of the entangled photon pair **103**. The objective **117** was a 0.4 microscope objective lens that received the photon pair **103**, and the scanner **110** and lenses were able to scan the beam angle of the photon pair at the overfilled back aperture of the 0.4 NA microscope objective lens.

[0058] To perform imaging of the sample **102**, the focus of the objective **117** was raster scanned by galvo mirrors of the scanner **110** across the sample **102**. The excitation light beam (i.e., beam having the entangled photon pair **103**) was to the objective by the dichroic beam splitter **114** (DMSP750B, Thorlabs Inc.) having a high reflectance at 800 nm. The fluorescence **104** from the sample **102** was visible light that was epi-collected by the objective **117** and passed through the dichroic beamsplitter **114** that was transparent to the visible fluorescence **104**. The fluorescence **104** propagated through two filters (FF02-409/LP, Semrock Inc. and 750 nm, OD 4 Shortpass Filter, Edmund Optics) that filtered out scattered light at 400 nm and 800 nm. The detector **112** was a cooled photo-multiplier tube (PMT) (R7518P, Hamamatsu Photonics). The fluorescence **104** was detected by the detector **112** and the detector provided a signal indicative of the detected fluorescence to a data acquisition device. The data acquisition and scanner control were implemented using a DAQ card (NI PXIe6341, National Instruments Corp.) and Scanimage (Vidrio Technologies Inc.) software.

[0059] The alignment of the output beam of entangled photon pairs **103** from the entangled photon source **105** was optimized to provide the photon pairs **103** to the system **100**. A focusing lens for the SPDC pump was chosen to obtain the highest output of the specific type of SPDC generated photon pairs. The focusing lens had the focal length of 10 cm, and the position of a collimating lens with a focal length of the collimating lens was tuned to match the size of an intersection area of ordinary and extraordinary cones of the SPDC with the size of the input aperture of the microscope scanner which was 4 mm. The BBO crystal was aligned to produce collinear and degenerated SPDC. FIG. **3**A is an image of the output transverse beam profile characteristic for the type-II SPDC configuration as captured by a CCD camera installed at an output port of the entangled photon source **105**.

[0060] The angle of the BBO crystal was tuned to provide a maximum cone intersection in collinear geometry. FIG. **3**B is an image captured by a CCD camera at the output port of the entangled photon source **105** with a maximally overlapped collimated SPDC beam (i.e., photon pair beam). The size and position of the cones intersect area was matched with the size and position of an input aperture of the system **100** by adjusting the collimating lens. Using the two-photon excitation of the microscopy system **100** the optical elements (e.g., scanner **110**, objective **117**, beam splitter **114**, other lenses, filters, etc.) were adjusted and test images of thin films of substances were obtained. FIG. **4** is a plot showing the absorbance and fluorescent spectra of bis-(styryl)benzene derivative Bu_2/OMe as obtained by the constructed ETPA microscopy system **100**. Bu_2/OMe is a substance that exhibits strong two-photon absorption fluorescence, which is why it was chosen as a test target as the sample **102**.

[0061] The constructed microscopy system **100** was capable of imaging at very low fluorescence signals below 1 photon/s. FIG. **5**A is an image of Bu_2/OMe in a drop cast film generated by the ETPA microscopy system **100** with an excitation flux of 10^7 photons/s, and FIGS. **5**B-**5**D are an image of the same Bu_2/OMe in the drop cast film captured by a classical light TPA microscopy system with excitation fluxes of 0.96×10^{12}, 0.96×10^{13}, 5×10^{13} photons/s respectively. The photon count rate of the provided excitation photons (i.e., for classical TPA microscopy and for the ETPA microscopy) were measured and maximized by adjusting the beam direction of the entangled photon source **105**, the scanner optics (i.e., scanner **220** and associated lenses/mirrors), and tube lenses. The photon count rate at the position of the objective **117** was compared with the photon count rate at an entrance to the scanner **110**. The highest photon count rate at the objective **117** was approximately 6×10^6 photons/s, which corresponds to an SPDC output beam coupling efficiency (i.e., the ratio of the excitation flux at the sample **102** to the flux at the entrance to the scanner **110**) **105** of 0.46.

[0062] The image of FIG. **5**A using the entangled photon excitation flux on the order of 10^7 photons/s is compared with the image of FIG. **5**B, obtained with the classical two-photon excitation with intensity on the order of 10^{12} photons/s. The image of FIG. **5**B demonstrated a fluorescence image intensity on the dark noise level despite an excitation flux increase of five orders of magnitude greater than the ETPA image of FIG. **5**A. The reduced image visibility, despite the increase in excitation flux, demonstrates a substantial enhancement of the two-photon absorption efficiency when using highly correlated entangled photon pairs. The images of FIGS. **5**C and **5**D illustrate that the entangled photon flux image of FIG. **5**A generated an image of the same intensity, in photons/pixel, as that obtained with classical light having an average photon flux on the order of $1.2*10^{13}$ photons/s. The enhancement allows for using a sample probing light flux in an ETPA microscope six orders of magnitude (i.e., 10^6) lower than that used with classical light two-photon excitation. The reduction of the probing light intensity is an advantage of the ETPA microscope for various applications, and may be especially useful for imaging in biological applications.

[0063] A precise polarization-dependent optical delay line based on birefringent material wedges was implemented as the delay line **107** of FIG. **1**. The polarization-dependent

optical delay line enabled control of the relative delay between orthogonally polarized biphoton components with the accuracy of 0.02 fs per step of a motor of the delay line **107**. In embodiments, the delay line **107** may be capable of providing a temporal delay resolution of 0.2 fs, 0.5 fs, 1 fs, 2 fs, 5 fs, a resolution of less than 1 fs, a resolution of less than 1 ps, or another temporal resolution as required. The temporal delay line may be capable of providing delays of 0 seconds, 1 picoseconds, 5 picoseconds, between 0 and 5 picoseconds, between 0 and 10 picoseconds, between 5 and 50 picoseconds, between 0 and 1 nanoseconds, or longer than a nanosecond. The delay line was made from a pair of 25 mm×20 mm×15 mm crystalline quarts wedges, as further described in reference to FIG. **10**. The delay line **107** was capable of producing a variable temporal delay between orthogonally polarized biphoton components with an accuracy of 0.02 fs per incremental step of the motorized delay line.

[0064] The quantum interference effect in the ETPA microscopy system **100** was measured by imaging a bis[18]-annulene (BT) cast film sample with different delays applied by the delay line **107**. The macroscopic fluorescence of the BT sample showed a non-monotonic dependence on the delay time between biphoton components (i.e., signal and idler delay). The non-monotonic dependence of the fluorescence results from the quantum path interference effects for the entangled photon pair absorption, and further, the interference provided a strong indication of the entangled photon origin of the signal in the macroscopic experiment. FIG. **6** presents a series of images of microcrystalline aggregates of bis[18]-annulene in a cast film at different signal-idler delays as obtained by the ETPA microscopy system **100**. Microscope scanning regimes with relatively small number of pixels and moderate spatial resolution to collect sufficient amount of the fluorescence photons per pixel and reduce statistical error were implemented in capturing the images of FIG. **6**. For the images of FIG. **6**, a pixel resolution of 128×128 with the pixel dwell time 0.32 ms was used. At each delay time position, a series of 1000 image frames were collected and integrated with the total collection time, for a given time delay, of a few hours. The total collection time at each delay between two photons was about 2 hours. The total collection time the entire set of six delays was ~12 hours. The images of FIG. **6** were noisy even at long scanning times due to weak efficiencies of entangled photon induced fluorescence. Still yet, the images of FIG. **6** illustrate the dependence of the image structure and intensity on the signal to idler delay. The fluorescence intensity at particular positions of the sample **102** under the objective **117** showed non-monotonic dependence on the delay between the components of the biphoton pair.

[0065] To better demonstrate the non-monotonic dependence of the image feature on the signal-idler delay, FIG.**7** presents a set of differential images that were constructed by subtracting the image $I_{\tau i}$ obtained with time delay τ_i from an image $I_{\tau k}$ obtained with a time delay τ_k keeping k−i=1. After normalizing to the background, the differential images showed the apparent signal sign reversal for particular image areas when the signal-idler delay was gradually increased from 0 to 120 fs. The sign reversal in differential images is illustrative of the non-monotonic character of the dependence of the ETPA fluorescence on the signal-idler delay, which is specific to the ETPA process. The difference between each set of two images was normalized to a value of positive 1 for positive differential values, and negative 1 for negative differential values. Therefore, a value of positive 1 or negative 1 represents a maximum or minimum of constructive interference of the entangled two-photon process, and not an interference between the components of bi-photon pairs.

[0066] The theoretical modeling of the ETPA is a challenging task even for small organic molecules. Reasonable predictions on the non-monotonic dependence of the ETPA process may be made using only the dominant pathway's energies. The BT molecule did not show an appreciable charge transfer character, and in the modeling of the ETPA, permanent dipole pathways may be neglected in virtual-state two-photon excitation pathways. Typically, there are intermediate energy levels between a ground state and a two-photon excited state of a molecule. As described herein, intermediate levels may also be referred to as virtual states or virtual energy states. The entangled photon absorption process can be described by using an intermediate level with high probability transition moments. The term "dominant pathway", as used herein, refers to a two-photon excitation process in a molecule according to a pathway through excitation of a single high probability transition moment intermediate level (i.e., a transition pathway having a high probability of population or a high probability of excitation via the pathway). FIG. **8**A is a diagram of the BT molecule used in the ETPA imaging herein. FIG. **8**B is an energy band diagram of the BT molecule assuming a single dominant intermediate level in a two-photon transition with a monochromatic pump at frequency ω_p. The delay time dependence of the ETPA cross-section σ_e may be determined by

$$\sigma_e = \frac{\pi\omega_p^2}{16A_eT_e}\delta(\epsilon_f-\epsilon_g-\epsilon_p)\left(\frac{\mu_{gi}\mu_f}{\Delta}\right)\times [4.5-4\cos(\Delta T_e)\cos(\Delta\tau)+0.5\cos(2\Delta\tau) \quad \text{EQ. 1}$$

where A_e and T_e are entanglement area and entanglement time, respectively, ϵ_g and ϵ_f are the energy of a ground and excited state, respectively, $\Delta=\epsilon_i-\epsilon_g-\omega_p/2$ is the detuning energy for an intermediate state having an energy ϵ_i, and μ_{gi} and μ_{if} are transition dipole matrix elements for gi and if state transitions, as illustrated in FIG. **8**B. Using EQ. 1, the fluorescence may be used to monitor the excited state population created by entangled photon pairs. The fluorescence may originate from relaxation from the excited state to a lower energy state, and therefore may not be affected by the non-classical nature of the excitation light in any way other than by the population of the excited state.

[0067] FIGS. **9**A and **9**B are plots of signal counts per pixel and a fit of theoretical fluorescence dependence on signal-idler delay according to EQ. 1 at two different pixel locations. In generating the theoretical fit, a product of the transition dipole matrix elements μ_{gi} and μ_{if}, and the detuning Δ, were adjustable parameters in the fitting procedure. The detuning parameter Δ was determined to have different values at different locations of the sample (i.e., at different pixels of an image). The plots of FIGS. **9**A and **9**B show data from two different sample locations having the coordinates X=30, Y=65 and X=73, Y=63, respectively, in pixels numbers for 128×128 pixel images. The detuning parameter was estimated to be $1.53*10^{14}$ s^{-1} and $0.88*10^{14}$ s^{-1}, respectively for the images of FIGS. **9**A and **9**B. While the

detuning parameters Δ□for different positions on the sample vary, they are similar, by an order of magnitude, to the detuning parameter $\Delta=0.78*10^{14}$ s^{-1} obtained in macroscopic experiments with the same BT molecule in a liquid solution.

[0068] The non-monotonic delay fluorescent image dependence illustrated by FIGS. **7**, **9**A, and **9**B results from quantum interference effects associated with the entanglement of the generated photon pairs and is not observable or exhibited by, classical light. The specific delay dependence provides an indication that images observed in the ETPA microscopy systems described herein are selectively produced by the entangled photon pairs. The drop cast film of the BT imaged by the ETPA microscope system **100** contains aggregates of the BT as well as isolated molecules. The aggregates of different structural arrangements (e.g. J-type, H-type, more complex such as herringbone-type structures) have different electronic properties (e.g., transition moments, energy level positions, etc.). It is expected that characteristics of the delay time dependence (e.g., period, modulation depth, visibility, etc.) should be different for different aggregates in a drop cast sample due to different energy level characteristics at different locations of the sample.

[0069] FIG. **10** is a diagram of an embodiment of a system **1000** for performing ETPA microscopy as described herein. The system **1000** may substantially be implemented as the ETPA system **100** of FIG. **1**, but the illustration of FIG. **10** includes additional elements and details. The system **1000** includes a microscopy unit **1010**, an SPDC unit **1040**, and a pump generation unit **1070**. The microscopy unit **1010** includes a plurality of optical and mechanical elements for performing scanning microscopy and capturing images of a sample **1012**. The SPDC unit **1040** includes a downconversion element **1042** and associated optics for generating SPDC and providing an SPDC beam **1047** of entangled photon pairs to the microscopy unit **1010**, and the pump generation unit **1070** includes a radiation source **1075**, a nonlinear element **1072**, and associated optical elements for generating pump radiation **1077**.

[0070] The pump generation unit **1070** includes the radiation source **1075** that is configured to provide pump radiation **1076** to a second harmonic generation (SHG) medium **1072**. In a constructed embodiment of the system **1000**, the radiation source **1075** was a mode-locked Ti:Sapphire laser (Mai Tai, Spectra Physics, Inc.) configured to provide the pump radiation **1076**, with the pump radiation **1076** being femtosecond pulsed pump radiation having a central wavelength of 800 nm. One or more lenses **1073** were configured to focus the pump radiation **1076** into the SHG medium **1072** to convert the pump radiation **1073** to second harmonic radiation **1078** pulses having a central wavelength of 400 nm. In embodiments, the SHG medium **1072** may include barium borate (BBO), periodically-poled (PPLN), unpoled lithium niobate, periodically poled potassium titanyl phosphate (PPKTP), unpoled potassium titanyl phosphate (KTP), or another nonlinear material or medium. A lens **1073** and dichroic mirror **1080** direct the second harmonic radiation **1078** output pulse towards the downconversion element **1042**. Residual pump radiation **1076***a* passes through the dichroic mirror **1080** and is blocked by a beam blocker **1079***a* to dispose of the residual pump radiation **1076***a*. A prism **1082** and interference filter **1085** are used to further separate the second harmonic radiation **1078** from the fundamental pump radiation **1076** resulting in a beam of second residual pump radiation **1079***b*. A second beam blocker **1079***b* is disposed to block the second residual pump radiation **1079***b*. Mirrors **1084** direct the second harmonic radiation **1078** through an aperture **1087** to provide the second harmonic radiation **1078** to the SPDC unit **1040**.

[0071] The SPDC unit **1040** received the second harmonic radiation **1078** from the pump generation unit **1070**. Two lenses **1043** were configured to focus the second harmonic generation **1043** into, collimate the radiation **1043** from, the downconversion element **1042**. A bandpass filter **1045** was disposed along the optical path, before the downconversion element **1042**, to further filter out undesired wavelengths of radiation from entering the downconversion element **1042**. The downconversion element **1042** converted the second harmonic radiation **1087** to SPDC photon pairs as the SPDC beam **1047**. In embodiments, the downconversion element may include one or more waveguides or bulk crystals of PPLN, bulk lithium niobate, PPKTP, BBO, or another nonlinear material or medium. In the embodiments being described, the downconversion element was a bulk BBO crystal. A dichroic mirror **1050** was disposed along the optical path configured to reflect residual second harmonic radiation **1078***a* which was detected by a photodetector **1052**. The photodetector **1052** provided a signal indicative of the detected residual second harmonic radiation **1078***a* to a processor **1090**. The processor **1090** may use the signal indicative of the detected residual harmonic radiation **1078***a* for determining an amount of generated photon pairs in the SPDB beam **1047**, measuring SPDC efficiencies, determining losses in the system **1000**, and/or for measuring and monitoring other metrics of the SPDC unit **1040** and pump generation unit **1070**. The SPDC beam **1047** passes through an aperture **1055** and an interference long pass filter **1058**, having a cut-on wavelength at 750 nm, was used to remove any remaining 400 nm second harmonic radiation.

[0072] A half wave plate **1060** was used to manipulate the polarizations of signal-idler pairs of photons of the SPDC beam **1047**, and a tunable delay line **1062** was disposed along the optical path to provide a relative temporal delay between the signal-idler photon pairs. The tunable delay line **1062** was a precise polarization-dependent delay line based on birefringent material wedges inserted between the downconversion element **1042** of the SPDC unit **1040** and the microscope input **1010**. The delay line **1062** included a pair of 25 mm×20 mm×15 mm crystalline quarts wedges. A first wedge was permanently fixed in place while a second wedge was mounted on a delay line stage that could translate the second wedge along an axis parallel to the long faces of the wedges (i.e., along the common diagonal direction of the diagonal faces of the first and second wedges as illustrated in FIG. **10**). Each component of an SPDC photon pair (i.e., the signal photon being a one component, and the idler photon being another component) has an orthogonal polarization relative to the other component of the photon pair. As such, the relative temporal delay between the two orthogonally polarized components was determined by the difference of corresponding refractive indexes of quartz for ordinary and extraordinary light, and the amount of quartz material of the tunable delay line **1062** that was in the light path. In order to compensate for the signal-idler delay produced in type-II BBO crystal (e.g., the downconversion element **1042**), and for the non-zero thickness of the wedged configuration of the delay line **1062** at minimum delay, a

pair of properly oriented crystalline quartz plates **1065** having thicknesses of 3.4 mm+2.0 mm were introduced in the optical path. The delay line used in the microscope measurements and imaging experiments described herein was capable of producing a variable temporal delay between orthogonally polarized biphoton components (i.e., signal-idler photon pairs) with an accuracy of 0.02 fs per step of the motorized delay line. Finally, the time delay photon pairs of the SPDC beam **1047** passed through an aperture **1068** before being provided to the microscopy unit **1010**.

[0073] To evaluate the performance of the SPDC unit **1040**, downconverted photos of the SPDC beam **1047** were measure by either a silicon avalanche photodiode (APD) coupled to single photon counting modules (Perkin-Elmer SPCM-AQR-13), or by a CCD camera (ST-402, SBIG Astronomical Instruments). The SPDC unit **1040** was able to produce $1.2*10^7$ photons/s output flux (singles) and showed a signal-idler coincidence rate up to $1.5*10^6$ coincidence counts/s. With type-II SPDC phase matching conditions of the BBO downconversion element **1042**, the signal (o-ray) and idler (e-ray) photons were generated at orthogonal polarizations. Polarization visibility measurements were performed using a 50/50 non-polarizing beamsplitter and two polarizers placed in two individual APD optical paths, one path for measuring the signal photons, and another path for measuring the idler photons. A polarization visibility of approximately 88.5% was measured. The results of the polarization visibility and coincidence rate measurements showed that a two-photon quantum state was generated in the collinear configuration type-II SPDC in 1 mm thick BBO crystal (i.e., the downconversion element **1042**).

[0074] The microscopy unit **1010** received the SPDC beam **1047** as excitation radiation for exciting the sample **1012** for imaging of the sample **1012**. A mirror **1015** directed the SPDC beam **1047** to a spatial scanner **1018**. The spatial scanner **1018** was configured to scan the transverse position of photons of the SPDC beam **1047** for probing different parts of the sample **1012** for imaging of the sample **1012**. In embodiments, the scanner **1018** may be a galvo-galvo scanner having galvo-mirrors and scanning lenses **1018** and **1019** configured to raster scan the SPDC beam **1047** across the sample **1012**. A dichroic beam splitter **1022** with high reflection at 800 nm directed the SPDC beam toward a microscope objective **1025** and the scanner **1018** scanned the SPDC beam **1047** across the objective **1025** at the overfilled back aperture. The objective **1025** was a 0.4 NA microscope objective lens, but it is envisioned that other microscope objectives having different magnifications and backfill apertures may be used. The objective **1025** focuses the SPDC beam **1047** onto the sample and the SPDC beam **1047** excites the sample **1012** causing the sample to fluoresce releasing fluorescent radiation **1033**. The fluorescent radiation **1033** from the sample **1012** was epi-collected by the microscope objective **1025** and dichroic beamsplitter **1022** transmitted the fluorescent radiation **1033**. Two filters (not illustrated, FF02-409/LP, Semrock Inc. and 750 nm, OD 4 Shortpass Filter, Edmund Optics) further filtered out any other noise or residual radiation and a lens **1027** focused the fluorescent radiation **1033** into a cooled photo-multiplier tube **1030** (PMT) (R7518P, Hamamatsu Photonics). The PMT **1030** detected the fluorescent radiation **1033** and provided a signal indicative of the detected fluorescent radiation **1033** to the processor **1090**.

[0075] In embodiments, the processor **1090** may be communicatively coupled to one or more elements of the system **1000**. For example, the processor **1090** may be in communication with the scanner **1018** to provide control of the scanner for performing raster scans of the sample **1012** (e.g., turning on/off the scanner **1018**, controlling a position of the scan of the scanner, etc.). The processor **1090** may also receive feedback from the scanner **1018** pertaining to a current scanning position of the scanner **1018**, an error, an operational status, a temperature, or another metric or operational parameter of the scanner **1018**. Further, the processor **1090** may be in communication with the PMT **1030**, photodiode **1052**, tunable delay line **1062**, and/or other components of the system **1000** for controlling elements of the system, and/or for receiving signals from the elements.

[0076] Using the system **1000** of FIG. **10**, ETPA fluorescence images of various organic cast film samples were obtained. FIGS. **11**A and **11**B are ETPA and classical TPA images, respectively, of a biz[18]annulene (BT) drop cast film having the molecular structure illustrated in FIG. **11**C. FIGS. **11**D and **11**E are ETPA and classic TPA images, respectively, of a flavin mononucleotide (FMN) drop cast film having the molecular structure illustrated in FIG. **11**F. FIGS. **11**G and **11**H are ETPA and classic TPA images, respectively, of a anicotinamide adenine dinucleotide (NADH) drop cast film having the molecular structure illustrated in FIG. **11**I. The ETPA images were obtained by collecting images in 128×128 square pixel frames and collecting between 1000 to 2000 frames for each image. The sum of the signals in each pixel was taken over all collected frames. The background signal, with the laser pump blocked, was found to be about 0.3-1 photons per pixel depending on the number of frames and microscope alignment conditions of the system **1000**. The ETPA-induced microscope fluorescence images obtained (i.e., FIGS. **11**A, **11**D, and **11**G) were compared with the images collected under weak classical one-photon and two-photon excitation at 400 nm (i.e., FIGS. **11**B, **11**E, and **11**H). For classical 800 nm two-photon measurements, we adjusted the fundamental coherent laser beam from Mai Tai femtosecond laser to the average flux level 10^{12}-10^{14} photons/s (sub-milliwatt range) in order to produce about the same fluorescence intensity detected by the microscope as that obtained with much weaker entangled photon excitation. The ETPA microscope images of FIGS. **11**A-**11**I required 1,000,000 times less excitation flux to obtain the images than the corresponding TPA images.

[0077] FIG. **12** is a flow diagram of a method **1200** for performing ETPA microscopy as described herein. For clarity, the method **1200** of FIG. **12** will be described with simultaneous reference to FIG. **1**. The method includes generating an entangled photon pair (block **1202**). The entangled photon pair may be generated by the entangled photon source **105**, or by another photon source. The method **1200** further includes providing the entangle photon pair to the delay line **107** and applying a temporal delay to the entangled photon pair (block **1204**). The delay line **107** may apply a different temporal delay to different components of the entangled photon pair (i.e., a signal photon and an idler photon). Therefore, the delay line **107** may provide a relative temporal delay between the photons of the entangled photon pair.

[0078] The entangled photon pair is then provided to the sample **102** (block **1206**). The photon pair may be directed

toward the sample **102** by various optics and by the scanner **110**. The scanner **110** may be configured to alter the trajectory of the photons of the entangled photon pair to provide the entangled photon pair to different regions or areas of the sample **102**. For example, the scanner **110** may include one or more mirrors that are able to alter the direction of the entangled photon pair to provide the photon pair to the sample **102** at different transverse locations of the sample **102**. In an embodiment, the scanner **110** may raster scan the entangled photon pair across the sample **102** in a transverse plane of the sample **102**.

[0079] The sample **102** absorbs the entangled photon pair and the sample **102** fluoresces. The detector **112** detects the fluorescence and generates a signal indicative of the fluorescence (**1208**). The detector **112** may be configured to provide the signal to a processor for further processing of the signal. For example, the detector **112** may be configured to provide the signal to the processor **1090** of FIG. **10**, and the processor **1090** may be configured to generate an image from the signal. The processor **1090** may receive a plurality of signals from the detector **112** with each signal being indicative of fluorescence detected with the fluorescence being emitted from one or more regions of the sample **102**. The processor **1090** may generate an image having pixels, with each pixel being indicative of fluorescence received from a region of location of the sample **102**. The processor **1090** may generate a plurality of images of the sample **102** and the processor may perform image processor to generate an image, store the image in a memory or on a network, and/or display the generated plurality of images to a user. For example, the processor **1090** may normalize each image to a background noise level of each image, and/or the processor may generate one or more differential images from the plurality of images with each differential image being the result of a differential process between two or more images of the plurality of images.

[0080] The ETPA microscopy system **1000** of FIG. **10** was used to image various organic molecules as the sample **1012**. FIG. **13** is a plot of ETPA fluorescence versus input flux of excitation entangled photon pair beams. The fluorescence is normalized to the maximum number of the detected fluorescence photons. The plot shows the linear dependence of the fluorescence of the molecules on the input flux in photons per second. The three organic molecules of FIG. **13** were bis-annulene (BT) in a drop cast film, thiophene dendrimer in chloroform solvent (OM 82C), and zinc tetraphenylporphyrin (ZnTPP). The ETPA cross section, OF, for the BT, OM 82C, and ZnTPP was 5.4×10^{-18} cm^2, 2.6×10^{-81} cm^2, and 8×10^{-18} cm^2, respectively. Further, the fluorescence quantum yield, taken as fluorescent flux divided by the input flux, was 0.45, 0.74, and 0.04 for the BT, OM 82C, and ZnTPP, respectively.

[0081] FIG. **14**A is a plot of normalized absorbed photon rate versus input flux for ETPA of an organic molecule, and FIG. **14**B is a plot of normalized absorbed photon ate versus input flux for classical TPA. By comparing the data presented in FIGS. **14**A and **14**B, it is apparent that ETPA requires an input flux that is ten orders of magnitude less than classical TPA to achieve a same photon absorption rate. Therefore, it is envisioned that in some embodiments of ETPA microscopy systems, images may be captured that require input fluxes that are ten orders of magnitude, or more, less than an image obtained by classical TPA microscopy. ETPA microscopy may also be useful for performing spectroscopy of samples. By controlling certain characteristics of entangled photons generated by SPDC, different energy levels of a sample may be probed, which other spectroscopic techniques are unable to achieve. The described control of the excited states may be useful for probing energy levels of molecules for spectroscopy, and for controlling photochemical reactions. Further, the described tuning of the probing energy of entangled photon pairs allows for characterizing of molecules that have virtual energy levels and excitation pathways that are otherwise unable to be probed using other two-photon absorption imaging methods.

[0082] FIG. **15** is an example energy band diagram **1500** of a molecule having a ground energy state, g, an excited energy state, e, and multiple virtual energy states, v_1 through v_5. The ground energy state has the lowest energy of the system, the excited energy state has the highest energy value of the system as illustrated, and the virtual states each have energy values between the energies of the ground and excited states with increasing energy values from v_1 to v_5. The diagram **1500** also includes a first absorption pathway **1503**, a second absorption pathway **1506**, and a third absorption pathway **1509**. The first absorption pathway **1503** excites the molecule to the excited state through virtual state v_1. An excitation of the molecule according to the first pathway **1503** may occur with an entangled photon pair having a specific entanglement time T_e. Further, the second and third absorption pathways each excite the molecule through virtual states v_2 and v_3 respectively, which may be accomplished with entangled photon pairs having different entanglement times as compared to a transition through the first pathway **1503**. Therefore, the previously described ETPA microscopy systems **100** and **1000** may tune the entanglement time of generated entangled photon pairs to probe the various energies of the virtual states. While illustrated as having a single excited energy, e, molecules and other materials may have different pathways that excite the molecule to different excited energy states. Probing of the virtual states illustrated in FIG. **15** is not possible using a classical TPA microscopy system or spectroscopy method.

[0083] FIG. **16**A is a plot of simulated excitation transition probability of a hydrogen atom versus signal-idler delay of an SPDC bi-photon pair. FIG. **16**A illustrates a non-monotonic dependence of the transition probability of the delay. The multiple minima and maxima of the transition probability are indicative of quantum interference due to detuning energies of the bi-photon pair which is due to the energies of the entangled photons and the entangled two-photon cross-section of the hydrogen being probed. FIG. **16**B is a plot of the Fourier transform of the time delay plot of FIG. **16**A. FIG. **16**B presents an entanglement cross section of the bi-photon pair versus detuning energy, which is derived from the frequency as derived by the Fourier transform. The peaks **1612**, **1614**, **1618**, **1622**, and **1626** are indicative of the virtual states illustrated in FIG. **15**. For example, the lowest peak **1612** has the lowest energy of approximately 5 eV, which is indicative of an excitation transition according to the first pathway **1503** via the first virtual state v_1. Accordingly, the second peak **1614** is indicative of excitations via the second pathway **1506**, the third peak **1618** is indicative of excitations via the virtual state v_3, the fourth peak **1622** is indicative of transitions via the path3way **1509**, and the fifth peak **1626** is indicative of transitions via the fifth virtual state v_5. Therefore, by tuning

the time delay of the entangled photon pair, the a specific virtual state may be probed for determining a presence of a fluorophore, or for monitoring a biological process. The plot of FIG. **16**B is one example of a fingerprint of an atom. The plot of FIG. **16**B may be considered a spectral profile in energy, or alternatively, the x-axis may be converted to frequency with each of the peaks **1612**, **1614**, **1618**, **1622**, and **1626** corresponding to different frequency spectral components of virtual state pathways of the hydrogen atom. While described in reference to a hydrogen atom, a fingerprint, spectral profile, or energy profile may be generated using the described methods and systems, for any atom, molecule, or material.

[0084] FIG. **17**A is a plot of entanglement cross section versus entanglement time, T_e, for ETPA in a thiophene dendrimer. The entanglement cross section was determined from the measured fluorescence transition probability of the thophene dendrimer at various signal-idler bi-photon entanglement times using EQ. 1. FIG. **17**B presents table **1750** of the measured experimental entanglement cross-section values determined from the data illustrated in the plot of FIG. **17**A, and the theoretically determined entanglement cross-section values for an entangled photon pair in the thiophene dendrimer. The table **1750** presents experimental and theoretical data for both a planar thiophene dendrimer, and a twisted thiophene dendrimer. The measured and theoretical values reported in the table **1750** show good agreement indicating that the described methods and systems are reliable according to the theory for probing of virtual states of molecules and for performing spectroscopy of molecules.

[0085] The described method and systems for performing ETPA microscopy enable the ability to generate a spectral fingerprint (also termed profile) of a molecule that is incapable by classical TPA, and other forms of microscopy or spectroscopy. This spectral fingerprint is formed of absorption of fluorescence corresponding to excitation pathways having different virtual energy states. Knowing a spectral fingerprint of a molecule, including its virtual state transition energies, allows for optimization of a microscopy of spectroscopy system to tune excitation energies of the system for identifying subsequent molecules based on their absorption profiles and for imaging of molecules. For example, determining a highly efficient virtual state excitation transition pathway allows for tuning of excitation photon energies to utilize the efficient pathway, therefore reducing the overall required input power of an excitation energy source. This may further allow for ETPA imaging of samples at even lower input flux values. The described ETPA microscopy and spectroscopy methods described herein may be useful for imaging of biological systems. For example, ETPA spectroscopy can be used to observe virtual energy transitions in flavoproteins, which is unable to be performed by classical TPA and other techniques. Further, the ETPA microscopy can image the flavoproteins at very small concentrations of the flavoproteins allowing for imaging of the flavoproteins without requiring introduction of additional chemicals or fluorescent probes, which can disturb and/or change the behavior of some biological systems.

[0086] FIG. **18** is a flow diagram of a method **1800** for determining a fingerprint of a molecule using ETPA spectroscopy as described herein. The method **1800** may be performed by the system **100** of FIG. **1**, the system **1000** of FIG. **10**, or by another ETPA microscopy system. The method **1800** includes generating an entangled photon pair (block **1802**). The entangled photon pair includes a signal photon and an idler photon. The entangled photon pair may be generated via spontaneous parametric downconversion, another nonlinear optical process, or by another means. The entangled photon pair is then provided to a temporal delay line (block **1804**). The temporal delay line may include a birefringent delay line, a freespace delay line, a fiber coupled delay line, or another element capable of providing a temporal delay between photons of a photon pair or a group of photons. The temporal delay line provides a temporal delay between the signal photon and the idler photon (block **1806**). The entangled photon pair is then provided to a fluorophore (block **1808**) to excite the fluorophore. The fluorophore may be excited to an excited state via a pathway of transitions utilizing one or more virtual states of the fluorophore. In embodiments, the fluorophore may have one or more virtual states and the fluorophore may be excited to an excited state via pathways that use one or more of the virtual states. Further, each pathway that utilizes a virtual state has an efficiency associated with the pathway indicative of a population probability of the virtual state. For example, each pathway may have an associated two-photon absorption efficiency. Once excited, the fluorophore de-excites emitting a fluorescence.

[0087] The method **1800** further includes detecting the fluorescence from the fluorophore (block **1810**). A detector such as a photomultiplier tube may be used to detect the fluorescence. A spectral fingerprint is then determined from the detected fluorescence (block **1812**). The spectral fingerprint includes one or more spectral components indicative of one or more virtual states of the fluorophore. In examples, the detector generates a signal indicative of the detected fluorescence and the detector may provide the signal to a processor. The processor may store the signal as data in a memory, on a network, or on another storage medium. The method **1800** may be performed multiple times and the tunable delay line may provide a different temporal delay for each time that the method **1800** is performed. The processor may collect a plurality of signals from the detector with each signal associated with fluorescence detected at a given temporal delay. As such, the processor may determine a two-photon absorption efficiency of the fluorophore at different temporal delays. Further, the fingerprint for the molecule may be generated from the determined two-photon absorption efficiency. For example, the fingerprint may be generated by taking a Fourier transform of the two-photon absorption efficiency, and spectral components such as frequency peaks in the Fourier transform, may be used to determine energies of virtual states of the fluorophore. Once generated, the processor may store the fingerprint in a memory or transmit the fingerprint to another system.

[0088] FIG. **19** is a flow diagram of a method **1900** for probing a fluorophore, either to perform microscopy of the fluorophore, or for performing spectroscopy of the fluorophore. The method **1900** includes obtaining a spectral fingerprint of a fluorophore (block **1902**). The fingerprint includes one or more spectral components indicative of one or more virtual states of the fluorophore. The spectral components may be used to determine an energy state of an entangled photon pair, or of a classical photon pair, for exciting the fluorophore via two-photon absorption. The method **1900** further includes, generating a photon pair according to a virtual energy state of the fluorophore, with

the photon pair having an energy determined from a spectral component of the fingerprint (block **1904**). The photon pair is then provided to a fluorophore, with the fluorophore having the obtained spectral fingerprint, to excite the fluorophore via two-photon absorption (block **1906**). The fluorophore then fluoresces and the fluorescence is detected (block **1908**). The fluorescence may be detected by a detector that generates a signal indicative of the detected fluorescence and provides the signal to a processor. The processor may further process one or more signals from the detector to generate an image of the fluorophore, or for generating a spectrum of the fluorophore. The method **1900** of FIG. **19** may be useful for performing low excitation energy imaging and spectroscopy of biological samples, flavoproteins, living samples, monitoring biological processes, and material samples as a means.

[0089] The following list of aspects reflects a variety of the embodiments explicitly contemplated by the present disclosure. Those of ordinary skill in the art will readily appreciate that the aspects below are neither limiting of the embodiments disclosed herein, nor exhaustive of all of the embodiments conceivable from the disclosure above, but are instead meant to be exemplary in nature.

[0090] Aspect 1. A fluorescence probing system comprising:

[0091] an entangled photon source to generate an entangled photon pair including an idler photon and a signal photon;

[0092] a temporal delay line disposed to create a temporal delay between the idler photon and the signal photon to generate a temporally delayed entangled photon pair;

[0093] a coupling stage positioned to probe a sample having a fluorophore with the temporal delayed entangled photon pair to excite a virtual state of the fluorophore; and

[0094] a photodetector to detect fluorescent light emitted by the fluorophore and generate a signal indicative of the detected fluorescent light.

[0095] Aspect 2. The system of aspect 1, wherein the temporal delay line comprises a birefringent delay line.

[0096] Aspect 3. The system of any of aspects 1 to 2, wherein the entangled photon source comprises a nonlinear optical medium and is to generate the entangled photon pair by spontaneous parametric downconversion.

[0097] Aspect 4. The system of any of aspects 1 to 3, wherein the entangled photon source is to generate the entangled photon pair comprising near-infrared photons.

[0098] Aspect 5. The system of any of aspects 1 to 4, wherein the temporal delay line is to provide a temporal delay of between 0 seconds and 5 picoseconds.

[0099] Aspect 6. The system of any of aspects 1 to 5, wherein the temporal delay line is to provide a temporal delay having a temporal resolution of less than 1 femtosecond.

[0100] Aspect 7. The system of any of aspects 1 to 6, wherein the detector comprises a photomultiplier tube.

[0101] Aspect 8. The system of any of aspects 1 to 7, further comprising a scanner configured to scan the entangled photon pair in a transverse plane across the sample.

[0102] Aspect 9. The system of any of aspects 1 to 8, further comprising a controller to adjust the temporal delay between the idler photon and the signal photon over a sampling time to generate a plurality of different temporally delayed entangled photon pairs over the sampling time, each of the plurality having a different temporal delay; and wherein the photodetector is to detect fluorescence light emitted by the fluorophore and generate signals indicative of a spectrum of energies of virtual states of the sample.

[0103] Aspect 10. The system of any of aspects 1 to 9, wherein the photodetector is to provide the signals indicative of the spectrum of energies of virtual states for the sample to a processor, and the processor is to execute machine readable instructions that, when executed, cause the processor to:

[0104] collect, from the detector, the signals indicative of the spectrum of energies of virtual states;

[0105] generate a spectral profile for the sample, the spectral profile comprising one or more spectral components corresponding to one or more virtual states of the sample; and

[0106] storing the spectral profile.

[0107] Aspect 11. The system of any of aspects 1 to 10, wherein the detector is to provide the signal indicative of the fluorescent light to a processor, and the processor is to execute machine readable instructions that, when executed, cause the processor to:

[0108] collect, from the detector, the signal indicative of the fluorescent light; and

[0109] generate an image comprising a plurality pixels, each pixel being indicative of a received signal from the detector, and each pixel having a corresponding location in the transverse plane of the sample.

[0110] Aspect 12. A method for performing fluorescence microscopy, the method comprising:

[0111] providing, by an entangled photon source, an entangled photon pair to a temporal delay line, wherein the entangled photon pair includes a signal photon and an idler photon;

[0112] providing, by the temporal delay line, a delay to the entangled photon pair to create a relative temporal delay between the signal photon and the idler photon;

[0113] providing the entangled photon pair to a sample, wherein the sample absorbs the entangled photon pair and emits fluorescence;

[0114] detecting, by a detector, the fluorescence; and

[0115] generating, by the detector, a signal indicative of the detected fluorescence.

[0116] Aspect 13. The method of aspect 12, wherein the temporal delay line comprises a birefringent delay line.

[0117] Aspect 14. The method of any of aspects 12 to 13, wherein the entangled photon source comprises a nonlinear optical medium configured to generate spontaneous parametric downconversion entangled photon pairs.

[0118] Aspect 15. The method of any of aspects 12 to 14, wherein the entangled photon pair comprises near-infrared photons.

[0119] Aspect 16. The method of any of aspects 12 to 15, wherein the temporal delay line provides a temporal delay having a temporal resolution of less than 1 femtosecond.

[0120] Aspect 17. The method of any of aspects 12 to 16, further comprising scanning, by a scanner, the entangled photon pair to provide the entangled photon pair to different regions of the sample in a transverse plane of the sample.

[0121] Aspect 18. The method of any of aspects 12 to 17, wherein the detector is configured to provide the signal indicative of the fluorescent light to a processor, and the method further comprises:

[0122] collecting, by the processor, the signal indicative of the fluorescent light from the detector; and

[0123] generating, by the processor, an image comprising a plurality pixels, each pixel being indicative of a received signal from the detector, and each pixel having a corresponding location in the transverse plane of the sample.

[0124] Aspect 19. The method of any of aspects 12 to 18, further comprising:

[0125] generating, by the processor, a plurality of images, each image comprising a plurality of pixels with each pixel being indicative of a received signal from the detector; and

[0126] generating, by the processor, a differential image from at least two images of the plurality of images.

[0127] Aspect 20. The method of any of aspects 12 to 19, further comprising, before generating the differential image, normalizing, by the processor, two or more images of the plurality of images to a background of each of the two or more images.

[0128] Aspect 21. A method for generating a spectral fingerprint of a sample, the method comprising:

[0129] generating an entangled photon pair;

[0130] providing the entangled photon pair to a temporal delay line, wherein the entangled photon pair includes a signal photon and an idler photon;

[0131] providing, by the temporal delay line, a delay to the entangled photon pair to create a relative temporal delay between the signal photon and the idler photon;

[0132] providing the entangled photon pair to a fluorophore to excite the fluorophore via an excitation pathway having a virtual state of the fluorophore;

[0133] detecting fluorescence of the fluorophore;

[0134] generating a spectral fingerprint of the fluorophore, the spectral fingerprint including one or more spectral components indicative of one or more virtual states of the fluorophore.

[0135] Aspect 22. A method according to aspect 21, wherein the entangled photon pair is generated via spontaneous parametric downconversion.

[0136] Aspect 23. A method according to either aspect 21 or aspect 22, wherein the temporal delay line comprises a birefringent delay line.

[0137] Aspect 24. A method according to any of aspects 21 to 23, wherein the entangled photon pair comprises near-infrared photons.

[0138] Aspect 25. A method according to any of aspects 21 to 24, wherein the temporal delay line provides a temporal delay having a resolution of less than 1 femtosecond.

[0139] Aspect 26. A method according to any of aspects 21 to 25, wherein the temporal delay line provides a temporal delay of between 0 and 5 picoseconds.

[0140] Aspect 27. A method according to any of aspects 21 to 26, further comprising:

[0141] controlling the temporal delay of a plurality of entangled photon pairs, each pair of the plurality of entangled photon pairs having a different temporal delay;

[0142] providing each pair of entangled photons of the plurality of entangled photon pairs to the fluorophore to excite the fluorophore;

[0143] detecting fluorescence of the fluorophore due to the excitation of the fluorophore;

[0144] generating signals indicative of the detected fluorescence; and

[0145] determining the spectral fingerprint of the fluorophore, the spectral fingerprint including spectral components indicative of one or more virtual states of the fluorophore.

[0146] Aspect 28. A method according to any of aspects 21 to 27, further comprising: storing the spectral profile in a memory.

[0147] Aspect 29. A method for probing a fluorophore, the method comprising:

[0148] obtaining a spectral fingerprint of the fluorophore, the spectral fingerprint including one or more spectral components indicative of one or more virtual states of the fluorophore;

[0149] generating an entangled photon pair according to an energy of a virtual state of the fluorophore, the energy determined from a spectral component of the fingerprint;

[0150] providing the generated entangled photon pair to the fluorophore to excite the fluorophore via two-photon absorption; and

[0151] detecting fluorescence of the fluorophore.

[0152] Aspect 30. The method of aspect 29, further comprising, generating an image of the fluorophore from the detected fluorescence.

[0153] Aspect 31. The method of any of aspects 29 and 30 further comprising, determining a spectral component of the fluorophore from the detected fluorescence.

[0154] Throughout this specification, plural instances may implement components, operations, or structures described as a single instance. Although individual operations of one or more methods are illustrated and described as separate operations, one or more of the individual operations may be performed concurrently, and nothing requires that the operations be performed in the order illustrated. Structures and functionality presented as separate components in example configurations may be implemented as a combined structure or component. Similarly, structures and functionality presented as a single component may be implemented as separate components. These and other variations, modifications, additions, and improvements fall within the scope of the target matter herein.

[0155] Additionally, certain embodiments are described herein as including logic or a number of routines, subroutines, applications, or instructions. These may constitute either software (e.g., code embodied on a non-transitory, machine-readable medium) or hardware. In hardware, the routines, etc., are tangible units capable of performing certain operations and may be configured or arranged in a certain manner. In example embodiments, one or more computer systems (e.g., a standalone, client or server computer system) or one or more hardware modules of a computer system (e.g., a processor or a group of processors) may be configured by software (e.g., an application or application portion) as a hardware module that operates to perform certain operations as described herein.

[0156] In various embodiments, a hardware module may be implemented mechanically or electronically. For

example, a hardware module may comprise dedicated circuitry or logic that is permanently configured (e.g., as a special-purpose processor, such as a field programmable gate array (FPGA) or an application-specific integrated circuit (ASIC)) to perform certain operations. A hardware module may also comprise programmable logic or circuitry (e.g., as encompassed within a general-purpose processor or other programmable processor) that is temporarily configured by software to perform certain operations. It will be appreciated that the decision to implement a hardware module mechanically, in dedicated and permanently configured circuitry, or in temporarily configured circuitry (e.g., configured by software) may be driven by cost and time considerations.

[0157] Accordingly, the term "hardware module" should be understood to encompass a tangible entity, be that an entity that is physically constructed, permanently configured (e.g., hardwired), or temporarily configured (e.g., programmed) to operate in a certain manner or to perform certain operations described herein. Considering embodiments in which hardware modules are temporarily configured (e.g., programmed), each of the hardware modules need not be configured or instantiated at any one instance in time. For example, where the hardware modules comprise a general-purpose processor configured using software, the general-purpose processor may be configured as respective different hardware modules at different times. Software may accordingly configure a processor, for example, to constitute a particular hardware module at one instance of time and to constitute a different hardware module at a different instance of time.

[0158] Hardware modules can provide information to, and receive information from, other hardware modules. Accordingly, the described hardware modules may be regarded as being communicatively coupled. Where multiple of such hardware modules exist contemporaneously, communications may be achieved through signal transmission (e.g., over appropriate circuits and buses) that connect the hardware modules. In embodiments in which multiple hardware modules are configured or instantiated at different times, communications between such hardware modules may be achieved, for example, through the storage and retrieval of information in memory structures to which the multiple hardware modules have access. For example, one hardware module may perform an operation and store the output of that operation in a memory device to which it is communicatively coupled. A further hardware module may then, at a later time, access the memory device to retrieve and process the stored output. Hardware modules may also initiate communications with input or output devices, and can operate on a resource (e.g., a collection of information).

[0159] The various operations of example methods described herein may be performed, at least partially, by one or more processors that are temporarily configured (e.g., by software) or permanently configured to perform the relevant operations. Whether temporarily or permanently configured, such processors may constitute processor-implemented modules that operate to perform one or more operations or functions. The modules referred to herein may, in some example embodiments, comprise processor-implemented modules.

[0160] Similarly, the methods or routines described herein may be at least partially processor-implemented. For example, at least some of the operations of a method may be performed by one or more processors or processor-implemented hardware modules. The performance of certain of the operations may be distributed among the one or more processors, not only residing within a single machine, but deployed across a number of machines. In some example embodiments, the processor or processors may be located in a single location (e.g., within a home environment, an office environment or as a server farm), while in other embodiments the processors may be distributed across a number of locations.

[0161] The performance of certain of the operations may be distributed among the one or more processors, not only residing within a single machine, but deployed across a number of machines. In some example embodiments, the one or more processors or processor-implemented modules may be located in a single geographic location (e.g., within a home environment, an office environment, or a server farm). In other example embodiments, the one or more processors or processor-implemented modules may be distributed across a number of geographic locations.

[0162] Unless specifically stated otherwise, discussions herein using words such as "processing," "computing," "calculating," "determining," "presenting," "displaying," or the like may refer to actions or processes of a machine (e.g., a computer) that manipulates or transforms data represented as physical (e.g., electronic, magnetic, or optical) quantities within one or more memories (e.g., volatile memory, non-volatile memory, or a combination thereof), registers, or other machine components that receive, store, transmit, or display information.

[0163] As used herein any reference to "one embodiment" or "an embodiment" means that a particular element, feature, structure, or characteristic described in connection with the embodiment is included in at least one embodiment. The appearances of the phrase "in one embodiment" in various places in the specification are not necessarily all referring to the same embodiment.

[0164] Some embodiments may be described using the expression "coupled" and "connected" along with their derivatives. For example, some embodiments may be described using the term "coupled" to indicate that two or more elements are in direct physical or electrical contact. The term "coupled," however, may also mean that two or more elements are not in direct contact with each other, but yet still co-operate or interact with each other. The embodiments are not limited in this context.

[0165] Those skilled in the art will recognize that a wide variety of modifications, alterations, and combinations can be made with respect to the above described embodiments without departing from the scope of the invention, and that such modifications, alterations, and combinations are to be viewed as being within the ambit of the inventive concept.

[0166] While the present invention has been described with reference to specific examples, which are intended to be illustrative only and not to be limiting of the invention, it will be apparent to those of ordinary skill in the art that changes, additions and/or deletions may be made to the disclosed embodiments without departing from the spirit and scope of the invention.

[0167] The foregoing description is given for clearness of understanding; and no unnecessary limitations should be understood therefrom, as modifications within the scope of the invention may be apparent to those having ordinary skill in the art.

1.-**20**. (canceled)

21. A method for analyzing a biological sample using fluorescence microscopy, the method comprising:

(a) generating, by an entangled photon source, an entangled photon pair comprising a signal photon and an idler photon;

(b) introducing the entangled photon pair to a temporal delay line to induce a relative temporal delay between the signal photon and the idler photon;

(c) directing the temporally delayed entangled photon pair into a biological sample comprising tissue or cells;

(d) inducing two-photon absorption within the biological sample, wherein the biological sample emits fluorescence in response to the entangled photon pair;

(e) detecting, by a photon-sensitive detector, fluorescence emitted from the biological sample;

(f) generating a signal indicative of one or more spatial or molecular properties of the biological sample based on the detected fluorescence; and

(g) analyzing the signal to assess structural, functional, or molecular characteristics of the biological sample.

22. The method of claim **21**, wherein the temporal delay line comprises a birefringent delay line.

23. The method of claim **21**, wherein the entangled photon source comprises a nonlinear optical medium configured to generate spontaneous parametric downconversion entangled photon pairs.

24. The method of claim **21**, wherein the entangled photon pair comprises near-infrared photons.

25. The method of claim **21**, wherein the temporal delay line provides a temporal delay having a temporal resolution of less than 1 femtosecond.

26. The method of claim **21**, further comprising scanning, by a scanner, the entangled photon pair to provide the entangled photon pair to different regions of the biological sample in a transverse plane of the biological sample.

27. The method of claim **21**, wherein the detector is configured to provide the signal indicative of the fluorescent light to a processor, and the method further comprises:

collecting, by the processor, the signal indicative of the fluorescent light from the detector; and

generating, by the processor, an image comprising a plurality pixels, each pixel being indicative of a received signal from the detector, and each pixel having a corresponding location in the transverse plane of the biological sample.

28. The method of claim **27**, further comprising:

generating, by the processor, a plurality of images, each image comprising a plurality of pixels with each pixel being indicative of a received signal from the detector; and

generating, by the processor, a differential image from at least two images of the plurality of images.

29. The method of claim **28**, further comprising, before generating the differential image, normalizing, by the processor, two or more images of the plurality of images to a background of each of the two or more images.

30. The method of claim **21**, wherein the biological sample is a living sample.

31. The method of claim **21**, wherein analyzing the signal to assess structural, functional, or molecular characteristics of the biological sample comprises analyzing biological function occurring within the biological sample.

32. The method of claim **21**, wherein analyzing the signal to assess structural, functional, or molecular characteristics of the biological sample comprises analyzing molecular characteristics by determining a spectral fingerprint of a molecular within the biological sample.

33. The method of claim **21**, wherein analyzing the signal to assess structural, functional, or molecular characteristics of the biological sample comprises analyzing molecular structure within the biological sample.

* * * * *